

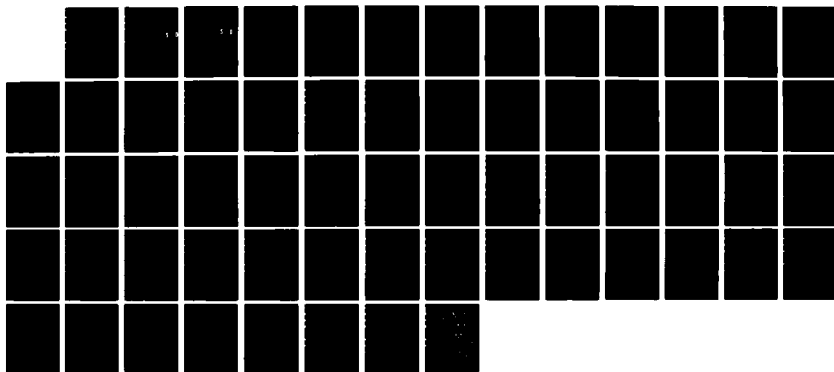
AD-A163 989

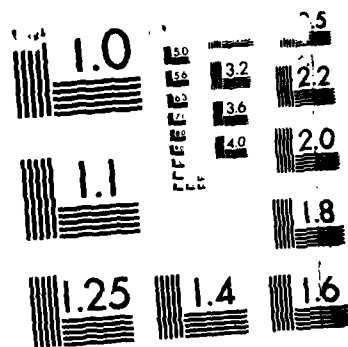
THE DETUMBLING OF AN AXIALLY SYMMETRIC SATELLITE WITH
AN ORBITAL MANEUVER (U) AIR FORCE INST OF TECH
WRIGHT-PATTERSON AFB OH SCHOOL OF ENGI K R FLEMING
13 DEC 85 AFIT/GA/AA/85D-5 F/G 22/2

1/1

UNCLASSIFIED

NL





MICROCOPY RESOLUTION TEST CHART
NATIONAL BUREAU OF STANDARDS 1963-A

AD-A163 989



DTIC
ELECTE
FEB 13 1986

S D
D

THE DETUMBLING OF AN AXIALLY SYMMETRIC
SATELLITE WITH AN ORBITAL MANEUVERING
VEHICLE BY NONLINEAR FEEDBACK CONTROL

THESIS

Kirk R. Fleming
First Lieutenant, USAF

AFIT/GA/AA/85D-5

DISTRIBUTION STATEMENT A

Approved for public release;
Distribution Unlimited

DEPARTMENT OF THE AIR FORCE
AIR UNIVERSITY

AIR FORCE INSTITUTE OF TECHNOLOGY

Wright-Patterson Air Force Base, Ohio

DTIC FILE COPY

1

AFIT/GA/AA/85D-5

DTIC
ELECTE
FEB 13 1986
S D

THE DETUMBLING OF AN AXIALLY SYMMETRIC
SATELLITE WITH AN ORBITAL MANEUVERING
VEHICLE BY NONLINEAR FEEDBACK CONTROL

THESIS

Kirk R. Fleming
First Lieutenant, USAF

AFIT/GA/AA/85D-5

Approved for public release; distribution unlimited

AFIT/GA/AA/85D-5

THE DETUMBLING OF AN AXIALLY SYMMETRIC SATELLITE
WITH AN ORBITAL MANEUVERING VEHICLE
BY NONLINEAR FEEDBACK CONTROL

THESIS

Presented to the Faculty of the School of Engineering
of the Air Force Institute of Technology
Air University
In Partial Fulfillment of the
Requirements for the Degree of
Master of Science in Astronautical Engineering

Kirk R. Fleming, B.S.
First Lieutenant, USAF

December 1985

Accession For	
NTIS CRA&I	<input checked="checked" type="checkbox"/>
DTIC TAB	<input type="checkbox"/>
Unannounced	<input type="checkbox"/>
Justification	
By	
Distribution /	
Availability Codes	
Dist	Avail and/or Special
A-1	

Approved for public release; distribution unlimited



Table of Contents

	Page
Acknowledgements	ii
List of Figures	iii
List of Tables	v
Abstract	vi
Notation	vii
I. Introduction	1
II. Problem Formulation	4
System Configuration	4
The Hooker-Margulies Equations	4
Application of the HM Equations	8
III. Nonlinear Feedback Control	13
IV. Results	20
V. Conclusion	46
References	48
Vita	49

Acknowledgments

I want to thank my thesis advisor, Lt. Col. Joseph W. Widhalin, for his guidance during the course of this project. I also owe special thanks to my classmates Robert Bandstra, William Berrier and Randall Richey for their helpful insight and comments, particularly with regard to my source code debugging efforts. I thank all my classmates for the support they gave me in this last, very busy quarter.

List of Figures

Figure	Page
1. The Conway and Widhalm Model for the Two Body Satellite . . .	2
2. The Five-Body Satellite Model	5
3. OMV Thrust Torques, Momentum Wheels Uncoupled	26
4. Universal Joint Torques, Uncoupled Momentum Wheels	26
5. Joint Position and Precession Angle Decay	27
6. Target Spin and Precession Angle Rate Decay	27
7. Constraint Loads at Universal Joint	28
8. Angular Velocities of OMV with u_7 and u_8 Feedback Only . . .	29
9. Angular Velocity of OMV with u_7 and u_8 Feedback Only . . .	29
10. Joint Constraint Loads, u_7 and u_8 Feedback Only	30
11. Control Torque History, u_7 and u_8 Feedback Only	30
12. Target Spin and Precession Angle Rates, u_7 and u_8 Feedback Only	31
13. Target Precession Angle and Joint Position, u_7 and u_8 Feedback Only	31
14. OMV Angular Velocity Components; Full Feedback Added at $t = 250$ seconds	32
15. OMV \hat{b}_3 Angular Velocity Component; Full Feedback Added at $t = 250$ seconds	32
16. Precession Angle Rate of Change and Target Spin Rate; Full Feedback Added at $t = 250$ seconds	33
17. Gimbal Control Torque u_7 With Full Feedback Added at $t = 250$ seconds	33
18. Control Torque u_8 and Constraint Torque T^C ; Full Feedback Added at $t = 250$ seconds	34
19. Constraint Force Magnitude and \hat{b}_2 Component; Full Feedback Added at $t = 250$ seconds	34

List of Figures, cont'd

Figure	Page
20. OMV Thruster Torques, \hat{b}_2 Momentum Wheel Torque Coupled to Target Precession Angle	35
21. \hat{b}_2 Momentum Wheel Control Torque, u_5 , and Wheel Angular Velocity; Control Torque u_5 Coupled to Target Precession Angle	35

List of Tables

Table	Page
I. Satellite Mass Properties	22
II. Initial Conditions	22
III. Gimbal Control and Constraint Torques, Uncoupled Momentum Wheels	36
IV. Gimbal Control and Constraint Torques, \hat{b}_2 Momentum Wheel Coupled	38
V. Momentum Wheel and Thruster Control Torques, \hat{b}_2 Momentum Wheel Coupled	40
VI. Gimbal Control and Constraint Torques, Gimbal Torque Feedback Only Until $t = 250$ seconds	42
VII. OMV Angular Velocity, Target Spin and Precession Angle Rate, Gimbal Torque Feedback Only Until $t = 250$ seconds	44

Abstract

The problem of detumbling a freely spinning and precessing axisymmetric satellite is considered. Detumbling is achieved with another axisymmetric orbital maneuvering vehicle (OMV) joined to the target satellite with a universal joint. The joint provides two rotational degrees of freedom and is translated across the surface of the OMV during the detumbling process. The target satellite and the OMV with its three momentum wheels are modelled as a five body system using Eulerian-based equations of motion developed by Hooker and Margulies. A Liapunov technique is applied to derive a nonlinear feedback control law which drives the system asymptotically to a final spin-stabilized state. State and control histories are presented and indicate that the dtumbling process is benign. Constraint force and moment loads at the connection between the OMV and target satellites are also presented, and indicate that no extreme loads are encountered during the despinning and detumbling process.

Notation

m_λ	= mass of body λ
m	= total system mass
Φ_λ	= inertia dyadic of body λ about its mass center
$\bar{\omega}_\lambda$	= angular velocity of body λ
\bar{F}_λ	= non-gravitational external force on body λ
\bar{T}_λ	= non-gravitational external torque on body λ
$\bar{\rho}_\lambda$	= geocentric position vector for mass center of body λ
$\bar{F}_{\lambda j}^H$	= interaction force acting on body λ through joint j
$\bar{T}_{\lambda j}^C$	= constraint torque acting on body λ through joint j
I	= unit dyadic
γ	= gravitational constant
$\bar{\rho}$	= geocentric position vector for system center of mass
$\hat{\rho}$	= unit vector in direction of $\bar{\rho}$
$\bar{T}_{\lambda j}^{SD}$	= spring-damper torque acting on body λ at joint j
\hat{g}_i	= unit vector along rotation axis of joint i
γ_i	= angle of rotation about axis \hat{g}_i
$\bar{\omega}_0$	= angular velocity of the reference body (the OMV)

THE DETUMBLING OF AN AXIALLY SYMMETRIC SATELLITE WITH AN ORBITAL MANEUVERING VEHICLE BY NONLINEAR FEEDBACK CONTROL

I. Introduction

The service or repair of orbiting satellites beyond direct reach of the Space Shuttle may require an orbital maneuvering vehicle (OMV) to rendezvous and dock with the target satellites. If the target is spin-stabilized it may be necessary to despin it. If the target has experienced control system malfunction or for some reason is not in pure spin, it may be necessary to detumble it. Docking followed by despinning or detumbling is defined here as capture. Docking is accomplished by first driving a grapple device on the OMV to a state of rest relative to some docking point on the target. The OMV and target can then be connected. Despinning or detumbling is accomplished by applying torques to the target through the connecting joint while firing the OMV thrusters to control the absolute motion of the two-body system. Widhalm and Conway derived a feedback control law (1) which solved the despinning/detumbling problem for the case of axisymmetric target and OMV satellites. They used a connecting joint which could translate across the surface of the OMV. The translational degree of freedom of the joint is depicted in Fig. 1 by the double arrow. The ability to translate the joint provides for joint position adjustment during docking, and allows the joint to be driven to the OMV axis of symmetry during detumbling. The resulting configuration can then be spin-stabilized.

This thesis extends the Widhalm and Conway model to include three orthogonal momentum wheels on the OMV, and develops a feedback control

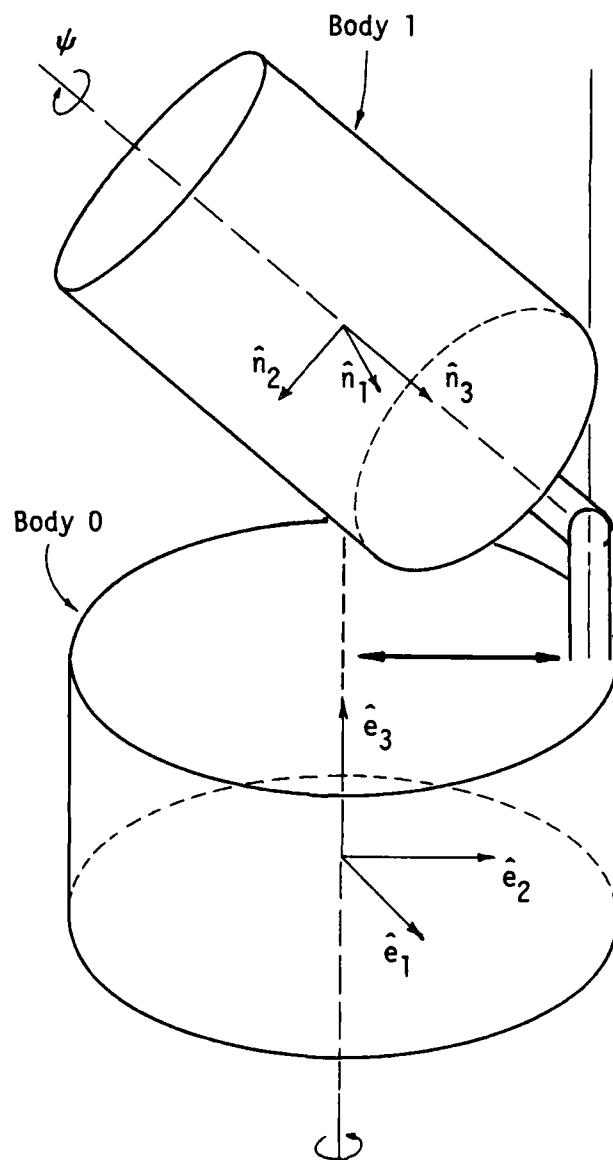


Fig. 1. The Conway and Widhalm Model for the Two Body Satellite

law to couple the momentum wheel torques to the system state. The target satellite docked with the OMV and its three momentum wheels are modelled as a system of five rigid, constant mass bodies. The control problem is formulated by defining the system initial configuration and the desired final state, and by deriving the equations of motion.

II. Problem Formulation

System Configuration

An axisymmetric target satellite is docked with an OMV which, with its three orthogonal momentum wheels, is also axisymmetric (see Fig. 2). The target and OMV are connected with a universal joint having two rotational degrees of freedom and the capability of translation across the surface of the OMV. The translational degree of freedom is depicted in Fig. 2 by the bold double arrow. The center of mass of the target lies on the \hat{b}_3 axis as does the mass center of the OMV-momentum wheel combination. The OMV is in a state of pure spin about \hat{b}_3 , and the target is in a state of spin with precession about \hat{b}_3 at a rate equal to the OMV spin rate. With no external moments or forces acting on the system a dynamically stable configuration results. This configuration represents the initial state of the system. The detumbling and despinning process is complete when the joint has been driven to a position lying on the \hat{b}_3 axis, and the target spin rate relative to the OMV is zero with the OMV itself still in a state of pure spin about the \hat{b}_3 axis. This configuration, or one arbitrarily close to it, represents the desired final state of the system. Both the initial and final states as defined imply that the initial and final angular velocities of the momentum wheels having rotational freedom about the \hat{b}_1 and \hat{b}_2 axes are zero. The initial and final angular velocity of the \hat{b}_3 wheel is arbitrary.

The Hooker-Margulies Equations

The dynamical attitude equations for a two-body satellite were derived by Fletcher, Rongved and Yu (2), and were generalized for an

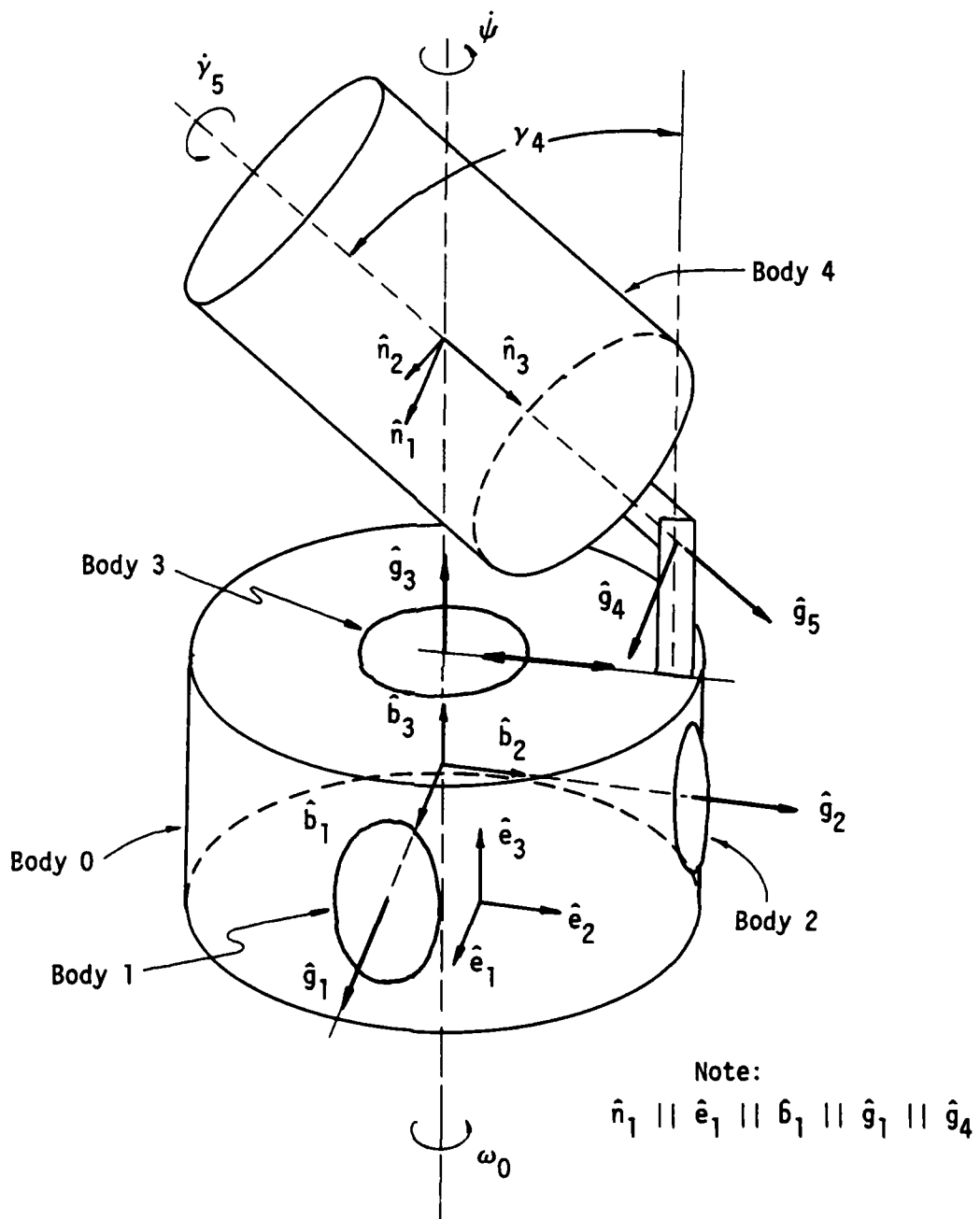


Fig. 2. The Five-Body Satellite Model

complete derivation is a set of $3n$ scalar equations for an n -body system. The equations are free of the unknown joint constraint forces, but still contain the unknown constraint torques (3:125).

Hooker (4) showed in a subsequent paper that the constraint torques could also be explicitly eliminated. The equations derived in reference (3) are written for all the bodies lying on one side of a selected joint and subsequently added. The interaction torques all cancel in pairs, with the exception of the constraint torque at the free joint. If the selected joint has a rotational degree of freedom about an axis g , the dot product of g and the expression just found for the torque is zero. Writing the dot product and setting it to zero yields an equation free of the constraint torque. Repeating the process for each degree of freedom at each joint eliminates all the unknown constraint torques and yields a system of r equations for an n -body system having r rotational degrees of freedom. These equations are referred to in some of the references as the modified Hooker-Margulies equations.

Although for an identical dynamical system a Lagrangian derivation would provide the same number of equations as the HM equations, the resulting expressions would not be written in terms of the physical body axes, as are the HM and modified HM equations. As a result adaptation to active control and modification to include effects such as joint motion would be more difficult (4:1205). The modified HM equations significantly reduce the required computer time for solution due to the reduction in the number of equations from $3n$ to r .

The constraint torques at the joints were eliminated explicitly by taking the dot product of the unit vector about which the joint is

n-body system by Hooker and Margulies (3). Both derivations assume that the bodies are connected by joints which are fixed with respect to the bodies they connect. In addition, the generalized Hooker-Margulies (HM) equations assume that the bodies are connected in a topological tree. This means that there are no closed loops formed by the interconnected bodies. The restriction of immovable joint is removed in an extension of the HM equations which will be discussed later. The extended equations then apply to the OMV-target satellite system when modelled as a system of five interconnected rigid bodies.

The derivation of the HM equations begins with the Newton and Euler equations for an n-body system. Each of the two sets of equations contains force terms representing the unknown constraint reactions which occur at the joints between adjacent bodies. An expression for each joint constraint force can be isolated by writing Newton's equations for all the bodies that lie to one side of any selected joint. The equations are added together, with the result that all the interaction forces cancel in pairs with the exception of the constraint force occurring at the selected joint. Repeating the process for all the joints in the system yields expressions for all the unknown constraints in terms of the system external forces and in terms of the inertial accelerations of each body in the system.

The joint constraint forces appear in Euler's equations as torques about the individual body mass centers, and can be replaced by the expressions for the constraints obtained in the process described. The result is the original Euler equations for the system, but with the unknown joint interactions explicitly eliminated. The result of the

free to rotate (there may of course be more than just one) with the summed vector dynamical equations for the bodies that lie to one side of that joint. The value of the constraint torque can be computed after the modified HM equations are solved, however. Given the system state, the derivatives of the state variables can be computed using the modified HM equations. All the variables in the equation which was dotted with the joint degree of freedom vector \hat{g} are then known, and can all be brought to one side of the equation with the resulting sum equalling the scalar components of the constraint torque (4:1207).

The interaction force at the joints can be computed by finding the acceleration of the mass center of the system of bodies lying to one side of a joint (relative to the system mass center) and multiplying by the total mass of that subsystem. For the case of no external forces, the product is the vector constraint force acting at the selected joint.

Application of the HM Equations

The Eulerian-based equations of motion for multi-body systems given by Hooker and Margulies (3) and modified by Hooker (4) are restricted to those systems of bodies connected in such a way that no closed loops are formed, and do not account for motion of the joints relative to the bodies adjacent to the joint. This last restriction was removed in an extension of the modified HM equations by Conway and Widhalm (5) to permit the translation of the joint across the face of the OMV. Thus the extended equations can be applied to the OMV, momentum wheels and target satellite system under consideration. Referring to Fig. 2 the OMV is labelled body 0, with the b basis fixed at its geometric center. The geometric center of the OMV is chosen to coincide with the center of mass

of the OMV-momentum wheel composite. That is, remove the target from the system and the system center of mass then lies at the origin of the \hat{b} frame. The momentum wheels lying on axes \hat{b}_1 , \hat{b}_2 , and \hat{b}_3 are labelled bodies 1, 2, and 3 respectively. The target satellite is body 4. The \hat{e} basis is fixed in body 0 at its mass center, and the \hat{n} basis is fixed in the target at its mass center. Since the target is precessing about its own angular momentum vector at a rate, $\dot{\psi}$, the OMV is positioned relative to the target so that the target's center of mass and angular momentum vector both lie on the \hat{b}_3 axis. The OMV is then spun about \hat{b}_3 at the same rate, $\dot{\psi}$, the target precession rate. The cone angle, γ_4 , and the distance from the target center of mass to the joint determine the required position of the joint on the OMV face for docking. The target's cone angle, γ_4 , precession rate, $\dot{\psi}$, spin rate, $\dot{\gamma}_5$, and mass properties are related as shown by Greenwood (6:386) and repeated here:

$$\dot{\psi} = I\dot{\gamma}_5 / (I_0 - I) \cos \gamma_4 \quad (1)$$

where I is the target's moment of inertia about the \hat{n}_1 and \hat{n}_2 axes and I_0 is the target's moment of inertia about the spin axis, \hat{n}_3 .

The two rotational degrees of freedom required at the universal joint include rotation, γ_4 , about an axis \hat{g}_4 parallel to \hat{b}_1 and rotation γ_5 , about an axis \hat{g}_5 parallel to \hat{n}_3 . The rotational degrees of freedom for the momentum wheels labelled 1, 2, and 3 are axes \hat{g}_1 , \hat{g}_2 , and \hat{g}_3 respectively. These three axes are parallel to the corresponding \hat{b} frame axes, with the wheel joints themselves taken to be at the mass centers of the wheels. From this initial docked configuration the problem is to drive the system to a final spin-stabilized state with a set of feedba

controls. This final state is specified by requiring the joint location to coincide with the \hat{b}_3 axis, and that the cone angle, γ_4 , and spin rate $\dot{\gamma}_5$, be reduced to steady state values of zero.

In the following equations of motion, all vectors and scalar rates are with respect to the \hat{e} basis fixed in the main body, the OMV. The attitude equations for the OMV-target satellite system can be derived directly from the extended equations given by Conway and Widhalm (5) and are:

$$\begin{bmatrix} a_{00} & a_{01} & . & . & . & a_{05} \\ a_{10} & a_{11} & . & . & . & . \\ . & . & . & . & . & . \\ . & . & . & . & . & . \\ . & . & . & . & . & . \\ a_{50} & . & . & . & . & . \end{bmatrix} \begin{bmatrix} \dot{\omega}_0 \\ \ddot{\gamma}_1 \\ \ddot{\gamma}_2 \\ \ddot{\gamma}_3 \\ \ddot{\gamma}_4 \\ \ddot{\gamma}_5 \end{bmatrix} = \begin{bmatrix} (m\bar{D}_{40} - m_4 \bar{L}_{40}) \times \bar{G} \\ \hat{g}_1 \cdot \bar{E}_1^* \\ \hat{g}_2 \cdot \bar{E}_2^* \\ \hat{g}_3 \cdot \bar{E}_3^* \\ \hat{g}_4 \cdot [\bar{E}_4^* + m\bar{D}_{40} \times \bar{G}] \\ \hat{g}_5 \cdot [\bar{E}_4^* + m\bar{D}_{40} \times \bar{G}] \end{bmatrix} \quad (2)$$

where

$$\begin{aligned} a_{00} &= \sum_{\lambda} \sum_{\mu} \phi_{\lambda\mu}, \text{ a dyadic} \\ a_{0k} &= \sum_{\lambda} \sum_{\mu} \epsilon_{k\mu} \phi_{\lambda\mu} \cdot \hat{g}_k, \text{ a vector} \\ a_{i0} &= \hat{g}_i \cdot \sum_{\lambda} \sum_{\mu} \epsilon_{i\lambda} \phi_{\lambda\mu}, \text{ a vector} \\ a_{ik} &= \hat{g}_i \cdot \sum_{\lambda} \sum_{\mu} \epsilon_{i\lambda} \epsilon_{k\mu} \phi_{\lambda\mu} \cdot \hat{g}_k, \text{ a scalar} \end{aligned} \quad (3)$$

$$\text{and } \epsilon_{i\mu} = \begin{cases} 1, & \text{if } \hat{g}_i \text{ belongs to a joint anywhere on the chain} \\ & \text{of bodies connecting } \mu \text{ and the reference body (0)} \\ 0, & \text{otherwise (e.g. if } \mu = 0) \end{cases}$$

and

$$\bar{G} = \ddot{D}_{04}^R + 2\bar{\omega}_0 \times \bar{D}_{04}^R \quad (4)$$

$$\phi_{\lambda\lambda} = \phi_{\lambda} + m_{\lambda} [\bar{D}_{\lambda}^2 1 - \bar{D}_{\lambda} \bar{D}_{\lambda}] + \sum_{\mu \neq \lambda} m_{\mu} [\bar{D}_{\lambda\mu}^2 1 - \bar{D}_{\lambda\mu} \bar{D}_{\lambda\mu}] \quad (5)$$

$$\phi_{\lambda\mu} = -m [\bar{D}_{\mu\lambda} \cdot \bar{D}_{\lambda\mu} 1 - \bar{D}_{\mu\lambda} \bar{D}_{\lambda\mu}] \quad (6)$$

$$\bar{D}_{\lambda} = - \sum_{\mu \neq \lambda} m_{\mu} m^{-1} \bar{L}_{\lambda\mu} \quad (7)$$

$$\bar{D}_{\lambda\mu} = \bar{D}_{\lambda} + \bar{L}_{\lambda\mu} \quad (8)$$

The vector $\bar{L}_{\lambda\mu}$ is the vector from the center of mass of body λ to the joint leading to body μ . \bar{E}_{λ}^* is determined from

$$\bar{E}_{\lambda}^* = \bar{E}_{\lambda} - \sum_{\mu} \phi_{\lambda\mu} \cdot \sum_k \epsilon_{k\mu} \dot{y}_k \dot{g}_k \quad (9)$$

and \bar{E}_{λ} is the vector

$$\begin{aligned} \bar{E}_{\lambda} = & 3\gamma\bar{\rho}^{-3} \hat{\rho} \times \phi_{\lambda\lambda} \cdot \hat{\rho} - \bar{\omega}_{\lambda} \times \phi_{\lambda\lambda} \cdot \bar{\omega}_{\lambda} + \bar{T}'_{\lambda} + \sum_{j \in J_{\lambda}} \bar{T}_{\lambda j}^{SD} \\ & + \bar{D}_{\lambda} \times \bar{F}'_{\lambda} + \sum_{\mu \neq \lambda} \bar{D}_{\lambda\mu} \times [\bar{F}'_{\mu} + m \bar{\omega}_{\mu} \times (\bar{\omega}_{\mu} \times \bar{D}_{\mu\lambda}) \\ & + m \bar{\rho}^{-3} (1 - 3\hat{\rho}\hat{\rho}) \cdot \bar{D}_{\mu\lambda}] \end{aligned} \quad (10)$$

In Eq (2) $\bar{\omega}_0 = \omega_{01}\hat{e}_1 + \omega_{02}\hat{e}_2 + \omega_{03}\hat{e}_3$, and the γ_i correspond to degrees of freedom about the unit vectors g_i . Superscript R implies that the indicated time differentiation is performed with respect to an observer fixed in the \hat{e} -frame. From Eqs (7) and (8) and from the definition given for $\bar{L}_{\lambda\mu}$, it is clear that the indicated time derivatives of \bar{D}_{04} are determined from the universal joint motion alone since the momentum wheel joints do not move with respect to the OMV. The joint motion is specified as are the control torques \bar{T}^{SD} in Eq (10). In this analysis, the external torques \bar{T}' are the three orthogonal thruster torques acting on the OMV, and all external forces are assumed zero. In addition, all gravitational terms are ignored (all terms containing the position vector $\bar{\rho}$). The way in which the control torques (including

thruster torques) and the joint motion is specified is covered in the next chapter.

The constraint forces and torques have been eliminated from the equations of motion as described earlier. These quantities can be determined by the methods described in references (3) and (4). The expressions for the constraint force and torque at the universal joint are:

$$\mathbf{F}_{04}^H = (m - m_4) \ddot{\mathbf{r}}_0 \quad (11)$$

$$\begin{aligned} \mathbf{T}_{41}^C = & (\boldsymbol{\phi}_{44} + \boldsymbol{\phi}_{40}) \cdot \dot{\boldsymbol{\omega}}_0 + (\boldsymbol{\phi}_{44} \cdot \hat{\mathbf{g}}_4) \ddot{\gamma}_4 \\ & + (\boldsymbol{\phi}_{44} \cdot \hat{\mathbf{g}}_5) \ddot{\gamma}_5 - \mathbf{E}_4^* - m\mathbf{D}_{40} \times \bar{\mathbf{G}} \end{aligned} \quad (12)$$

where $\bar{\mathbf{r}}_0$ is the position vector of the mass center of the OMV-momentum wheel combination, relative to the system center of mass, and where $\bar{\mathbf{G}}$ is as given in Eq (4).

III. Nonlinear Feedback Control

The detumbling and despinning problem presented here involves driving the universal joint connecting the OMV and target satellites across the face of the OMV to a point coincident with the \hat{b}_3 axis (see Fig. 2). Feedback control is used to maintain the attitude of the five-body system in such a way that the final state of the system is spin stabilized. The problem solution incorporates a feedback control approach in which an eight element control vector, \bar{u} , is a nonlinear function of the system state variables. In this chapter the eight controls are defined so that the equations of motion can be written in a simpler form more suitable for Liapunov analysis. This procedure closely parallels that described by Widhalm and Conway (7:6-9) in their derivation of a control law for the two-body satellite system described earlier. Liapunov's direct method is then used to derive a control law which is globally asymptotically stable with respect to the spin-stabilized equilibrium state.

Eq (2) is first written in the form

$$A \dot{\bar{x}} = \bar{F}^* \quad (13)$$

where A is defined as the 8×8 matrix on the left-hand side of Eq (2). The vector, \bar{F}^* , is defined as the eight element vector on the right-hand side of Eq (2), and

$$\begin{aligned} \dot{\bar{x}} &= [\dot{x}_1 \ \dot{x}_2 \ \dot{x}_3 \ \dot{x}_4 \ \dot{x}_5 \ \dot{x}_6 \ \dot{x}_7 \ \dot{x}_8]^T \\ &= [\dot{\omega}_{01} \ \dot{\omega}_{02} \ \dot{\omega}_{03} \ \ddot{\gamma}_1 \ \ddot{\gamma}_2 \ \ddot{\gamma}_3 \ \ddot{\gamma}_4 \ \ddot{\gamma}_5] \end{aligned} \quad (14)$$

Eq (14) is derived from the state variables

$$\begin{aligned}\bar{x} &= [x_1 \ x_2 \ x_3 \ x_4 \ x_5 \ x_6 \ x_7 \ x_8]^T \\ &= [\omega_{01} \ \omega_{02} \ \omega_{03} \ \dot{\gamma}_1 \ \dot{\gamma}_2 \ \dot{\gamma}_3 \ \dot{\gamma}_4 \ \dot{\gamma}_5]^T\end{aligned}\quad (15)$$

The control vector, \bar{u} , can be selected (7:6) so that Eq (13) can be written as

$$A \dot{\bar{x}} = \bar{F} + \bar{u} \quad (16)$$

Since the components of the vector, $\dot{\bar{x}}$, are the three angular acceleration components of the OMV, the three scalar angular accelerations of the orthogonal momentum wheels, and the angular accelerations of the target about the two degrees of freedom at the joint, the appropriate control vector components are apparent. The control vector, \bar{u} , is composed of three orthogonal (thruster) torques about each of the \hat{e} -basis vectors, three internal torques applied at the wheel axes, and finally two internal torques applied in the two degrees of freedom of the universal joint. These control torques are designated u_1 through u_8 , respectively. Premultiplying Eq (16) by the inverse of matrix A yields

$$\dot{\bar{x}} = A^{-1} \bar{F} + A^{-1} \bar{u} \quad (17)$$

since the matrix, A, will always be invertible for physical systems. The system of Eq (2) is augmented with the kinematical equation

$$\dot{x}_9 = x_7 \quad (18)$$

where x_9 is defined as the target precession angle, γ_4 , and completes the set of equations of attitude motion. We define the augmented state

vector, ${}_1\bar{x}_9$, to contain the vector, \bar{x} , plus the ninth element, x_9 .

To derive the control vector, \bar{u} , as a nonlinear function of the augmented state vector, ${}_1\bar{x}_9$, and the joint motion, a lemma presented by Vidyasagar (8) is applied. The lemma applies to autonomous systems, and the system of Eq (16) is nonautonomous because the OMV-target connecting joint motion is a specified function of time. Widhalm and Conway (7:7) have suggested that, by specifying the joint motion as a third order linear system which is asymptotically stable with respect to the desired final joint position, the third order system with Eqs (17) and (18) form an autonomous system. Since the desired final joint position relative to the \hat{b} -frame is given by the vector $[0 \ 0 \ c]$, and since the HM equations are written in terms of the \hat{e} -frame, we define the vector, \bar{c} , to be the vector leading from the origin of the b basis to the mass center of the OMV, the origin of the \hat{e} -frame. The scalar values that are to be driven to zero for asymptotically stable joint motion are the position, velocity, and acceleration components of the joint lying along the \hat{b}_2 axis. These scalars are given by:

$$\begin{aligned} (\bar{c} + \bar{L}_{04}) \cdot \hat{b}_2 &= y_1 \\ \dot{\bar{L}}_{04}^R \cdot \hat{b}_2 &= y_2 = \dot{y}_1 \\ \ddot{\bar{L}}_{04}^R \cdot \hat{b}_2 &= y_3 = \dot{y}_2 \end{aligned} \tag{19}$$

The derivative of the vector, \bar{c} , does not appear since the vector position of the OMV mass center relative to the geometric center of the OMV is constant. The complete autonomous system required for the application of the previously mentioned lemma is given by Eqs (17), (18), and (19)

and is formed by writing

$$\begin{aligned}\dot{\bar{x}} &= A^{-1} \bar{F} + A^{-1} \bar{u} \\ \dot{x}_9 &= x_7 \\ \dot{\bar{y}} &= D \bar{y}\end{aligned}\tag{20}$$

where D is a negative definite matrix selected to obtain the desired decay of the scalar y_1 given in Eq (19). The joint motion terms contained in the matrix, A , and in the vector, \bar{F} , are now specified by the vector \bar{y} leaving the system, (20), independent of time.

The lemma developed by Vidyasagar (8:157) in his discussion of Liapunov's direct method now applies to the system, (20), and is stated as follows: "Let $V({}_1x_9, y)$ be continuously differentiable and suppose that for some $d \geq 0$ the set

$$S_d^* = [{}_1\bar{x}_9, \bar{y} : V({}_1\bar{x}_9, \bar{y}) \leq d]$$

is bounded. Suppose that V is bounded below over the set S_d^* and that $\dot{V}({}_1\bar{x}_9, \bar{y}) \leq 0$ for all ${}_1\bar{x}_9$ and \bar{y} in S_d^* . Let S denote the subset of S_d^* defined by

$$S = [{}_1\bar{x}_9, \bar{y} \in S_d^* : \dot{V}({}_1\bar{x}_9, \bar{y}) = 0]$$

and let M be the largest invariant set of a system which is contained in S . Then whenever ${}_1\bar{x}_9(0)$ and $\bar{y}(0)$ are members of S_d^* , the solution of the system, (20), approaches M as $t \rightarrow \infty$."

Now M is an invariant set of system, (20), if every trajectory starting from an initial point in M remains in M for all time. Since the system, (20), is autonomous every trajectory through its state space is

an invariant set (8:156). The task then is to find a candidate Liapunov function, V , that meets the requirements of the lemma. To derive a non-linear feedback control law that drives the five-body system to the desired final state of spin-stabilized equilibrium, Widhalm and Conway (7) suggested a candidate Liapunov function like

$$V = (1/2) \bar{x}^T I \bar{x} + (1/2) K \dot{x}_9^2 + \bar{y}^T R \bar{y} \quad (21)$$

where I is the identity matrix, K is a positive constant, and R is a positive definite constant matrix. The function is continuously differentiable, and it is easy to select a vector ${}_1\bar{x}_9$ and a constant, d , to demonstrate that a set like S_d^* exists.

The condition on $\dot{V}({}_1\bar{x}_9, \bar{y})$ must be satisfied; differentiating V with respect to time yields

$$\dot{V} = \bar{x}^T I \dot{\bar{x}} + K \dot{x}_9 \dot{x}_9 + \dot{\bar{y}}^T R \bar{y} + \bar{y}^T R \dot{\bar{y}} \quad (22)$$

Substitution from the system, (20), gives the result

$$\begin{aligned} \dot{V} = & \bar{x}^T I [A^{-1} \bar{F} + A^{-1} \bar{u}] + K \dot{x}_9 \dot{x}_9 \\ & + \bar{y}^T [D^T R + R D] \bar{y} \end{aligned} \quad (23)$$

Now since R is a positive definite matrix and D was specified to be a negative definite matrix, then the expression $D^T R + R D$ is negative definite. Writing the Liapunov matrix equation

$$-Q = D^T R + R D \quad (24)$$

and defining

$$\dot{V}^* = - \bar{y}^T Q \bar{y} \quad (25)$$

implies both that Q is positive definite from Eq (24) and that as a result both V^* and $-\dot{V}^*$ are positive definite (8:172). Thus the third term in Eq (23) is negative definite. To make \dot{V} at least negative semi-definite, select the control vector

$$\bar{u} = -\bar{F} + A \begin{bmatrix} 0 & 0 & 0 & 0 & 0 & 0 & 0 & -Kx_9 & 0 \end{bmatrix}^T - A B \bar{x} \quad (26)$$

where the matrix B is positive definite or positive semi-definite. If the matrix B is positive definite, then V is negative semi-definite in x_9 . However, if the elements of B are positive except for $B_{33} = 0$, V is negative semi-definite in x_3 and x_9 . Then from the above lemma the system, (20), with control vector \bar{u} of Eq (26) is asymptotically stable with respect to the largest invariant set contained in the x_3, x_9 plane. But from Eq (26) it can be seen that any non-zero x_9 results in a non-zero control vector \bar{u} , which in turn causes a departure from the x_3, x_9 plane. Therefore the largest invariant set lies in the x_3, x_9 plane, but only in that region where x_9 is zero, namely the x_3 axis. The control vector \bar{u} of Eq (26) is then the desired nonlinear feedback control law for spin-stabilization of this system.

Non-zero off-diagonal terms must be included in the B matrix of Eq (26) which will couple the momentum wheel torques to state variables other than just the momentum wheel angular velocities. The torques must be coupled to the state variables in such a way that the angular rates of the \hat{g}_1 and \hat{g}_2 wheels decay to zero, so that the system stabilizes in pure spin. Implementing the control law of Eq (26) requires the determination of the non-zero elements of the matrix B , and the constant K . In their work with the two-body satellite system, Widhalm and Conway have suggested

that controls can be kept within reasonable limits by ensuring that the target center of mass does not depart appreciably from the \hat{b}_3 axis. This can be accomplished by selection of the matrix D, which controls the universal joint motion, in conjunction with K and the B_{77} element of the B matrix. Joint motion can be specified which will closely follow the decay of the target's precession angle, and maintain the proximity of the target mass center to the b_3 spin axis. Finally, substitution of the control vector \bar{u} of Eq (26) into Eq (20) yields the complete, linear system

$$\begin{aligned}\dot{\bar{x}} &= [0 \ 0 \ 0 \ 0 \ 0 \ 0 \ -Kx_9 \ 0]^T - B \bar{x} \\ \dot{x}_9 &= x_7 \\ \dot{\bar{y}} &= D \bar{y}\end{aligned}\tag{27}$$

From Eq (27) it can be clearly seen that if the matrix B is diagonal, and if the initial momentum wheel angular rates as well as the OMV angular velocity components ω_{01} and ω_{02} are zero, they will remain zero throughout the detumbling process. In the case where the only off-diagonal terms in B are those coupling the momentum wheel torques to selected system states, the ω_{01} and ω_{02} angular velocity components of the OMV still remain zero. This implies that throughout the maneuver the OMV remains in a state of pure spin.

IV. Results

In this chapter the basis for the selection of initial conditions and system mass properties is presented, as well as the values selected. System state histories and control torque histories are presented for four detumbling maneuvers. The four maneuvers include detumbling with feedback control without momentum wheel coupling, feedback control with a single momentum wheel coupled, detumbling using only gimbal (joint) torques, and finally, detumbling using only gimbal torques for the first 250 seconds, followed by 50 seconds of feedback control applying the full control torque vector with one wheel coupled. Representative histories for the constraint loads at the joint between the OMV and the target satellite are also given.

System mass properties were selected based on values used in previous research (9). The mass properties of the composite body consisting of the OMV and the three attached momentum wheels were selected to duplicate those of the OMV model used by Widhalm (9). Reasonable but arbitrary values of mass and moments of inertia were then selected for the three identical wheels. From this information and by specifying the location of the mass center of the composite OMV-momentum wheel system, the mass and inertia matrix for the OMV (without wheels) were computed. In this way direct comparisons could be made between the two-body and five-body analyses by completely decoupling the wheel control torques from all non-zero system states. As mentioned previously, this is accomplished by selecting all off-diagonal terms of the matrix B in the linear system (27) to be zero. Under this condition, the values of elements B_{44} , B_{55} , and B_{66} are completely arbitrary. In addition to the various mass

properties, the system state variable initial conditions were also duplicated from reference (9). The mass properties and initial conditions are given in Tables I and II, respectively.

From Eq (27) and from the discussion that immediately follows it, it can be seen that the values selected for elements B_{11} and B_{22} are also arbitrary, since they will always be multiplied by states x_1 and x_2 , which remain equal to zero throughout the detumbling, despinning maneuver. The values actually selected are those used by Widhalm (9) in the application of feedback control to the two-body satellite system. In that case states x_1 and x_2 attained non-zero values after approximately 290 seconds of open-loop control. Feedback control was then applied in an attempt to spin-stabilize the system, the desired response being obtained using the values $B_{11} = B_{22} = 0.046$.

The remaining constants to be determined include B_{77} , B_{88} , K , and the elements of the D matrix of the third order joint motion equation in Eq (27). Selecting the scalar equation from the 12 equation system of Eq (27) corresponding to the target precession angle motion, the constants B_{77} and K can be determined by specifying a desired final precession angle at the end of the maneuver. A total maneuver time of 300 seconds was selected, and critical damping specified. A final precession angle corresponding to the target mass center on the OMV spin axis and a final joint position equal to 0.05% of initial joint position was specified. The result obtained from these requirements is a solution with equal eigenvalues of about -0.035, with $B_{77} = 0.07$ and $K = 0.00123$. In a similar way, with the specification of the final joint position just given and with critical damping of the joint motion, equal eigenvalues

TABLE I

Satellite Mass Properties

	MASS	I_1	I_2	I_3
Target Satellite	1000 Kg	1000 Kg-m ²	1000 Kg-m ²	1100 Kg-m ²
OMV	4500 Kg	6400 Kg-m ²	6400 Kg-m ²	11800 Kg-m ²
Momentum Wheels	10 Kg	25 Kg-m ²	25 Kg-m ²	55 Kg-m ²

TABLE II

Initial Conditions

Variable	Meaning	Value
ω_{01}	\hat{e}_1 component OMV angular velocity	0.0
ω_{02}	\hat{e}_2 component OMV angular velocity	0.0
ω_{03}	\hat{e}_3 component OMV angular velocity	0.102
$\dot{\gamma}_1$	#1 momentum wheel spin rate	0.0
$\dot{\gamma}_2$	#2 momentum wheel spin rate	0.0
$\dot{\gamma}_3$	#3 momentum wheel spin rate	0.0
$\dot{\gamma}_4$	target precession angle rate	0.0
$\dot{\gamma}_5$	target spin rate	0.009
$(\bar{L}_{04} + \bar{c}) \cdot \hat{b}_2$	joint position	0.599
$\dot{\bar{L}}_{04} \cdot \hat{b}_2$	joint velocity	0.0
$\ddot{\bar{L}}_{04} \cdot \hat{b}_2$	joint acceleration	0.0
γ_4	target precession angle	0.349

Note: Values in TABLE II are given in meters, radians, or radians per second, as applicable.

of -0.04 were obtained for the joint motion equation. This resulted in values of $D_{31} = -0.000064$, $D_{32} = -0.0048$, and $D_{33} = -0.12$. Finally, solving the eighth scalar equation of the system of Eq (27) by requiring that the target spin rate be reduced to 0.5% of its initial value yields the value of $B_{88} = 0.02$.

With the momentum wheels uncoupled the system behavior was identical to that of the two-body system in Fig. 1, verified by the comparison of the results with those of Widhalm (9). Wheel torques were zero, with the OMV thrust torques and universal joint torques given in Figs. 3 and 4. None of these control torques reached large values, and it can be seen that the controls vary smoothly with time with no abrupt changes. The joint motion and precession angle decay behaved as specified, decaying to the small final values specified with no overshoot. The results are given in Fig. 5. The target spin rate decay displayed similar behavior. The precession angle rate of change and target spin rate histories are given in Fig. 6, where it can be seen that no radical motion has occurred. The constraint loads at the universal joint due to lack of rotational freedom and due to the loading required to drive the joint across the OMV were relatively small. The constraint torque maximum value was approximately 2 Nm, and the maximum force encountered in driving the joint was about 1 N. These results are shown in Fig. 7, where the magnitude of the constraint force is plotted, as well as the component of that force lying along the axis of joint motion. This b_2 component corresponds to the load capacity that would be required for a jackscrew, for instance, were such a device used on the OMV to obtain the desired joint motion.

Although global asymptotic stability is only guaranteed by the

lemma used earlier for the case of feedback control with the control law of Eq (26), it was of interest to attempt system despin and detumbling using only control torques applied at the universal joint. The result was that the system displayed no radical or unusual behavior, and approached a nearly spin-stabilized state after 300 seconds of control. The OMV still remained in a state closely approximating pure spin, although non-zero angular velocity components did remain. Figs. 8 and 9 show the OMV angular velocity history for this maneuver, and indicate that the departure from pure spin was modest. Constraint torque and interaction force at the connection also remained small, although as indicated in Figs. 10 and 11, a quasi-steady state condition was reached with continuous constraint and control torques experienced at the joint. A residual precession angle remained after the maneuver, but the rate of change of the precession angle was very small, indicating that the available control torques were able to maintain the system configuration but unable to change it at any appreciable rate. Although there was some oscillation in the precession angle rate of change, no other violent behavior occurred with respect to either target spin or precession angle changes. The results are shown in Figs. 12 and 13.

The maneuver described above was repeated, but at 250 seconds the full control vector was applied in an attempt to spin-stabilize the system. The residual non-zero ω_{02} component of the OMV angular velocity was reduced nearly to zero, and the OMV spin rate brought to a steady value (see Figs. 14 and 15). The relative spin rate of the target and the precession angle rate of change were likewise reduced to very nearly zero as indicated in Fig. 16. Although not plotted, the precession angle of

the target was reduced to half of its value at 250 seconds, or approximately 0.9 degrees. Figs. 17 through 19 show the attendant reductions in the constraint and control torques and in the constraint force at the joint. These data clearly indicate that the system is moving toward a spin stabilized equilibrium.

An attempt was made to couple the momentum wheels to the target precession angle rate and spin rate. The magnitude of the OMV thruster torque about each of the \hat{b} axes was integrated over the maneuver period, and the three resulting values added to obtain some measure of the total torque power required from the thrusters. The resulting total was then compared for maneuvers completed using various off-diagonal gain terms in the B matrix of Eq (26). No attempt at using control torque on the \hat{b}_3 wheel yielded a reduction in the OMV thruster torque requirements. Using applied torque at the \hat{b}_2 wheel by setting B_{57} to 1.0 resulted in a reduction of the integrated thrust torque from 436 Nm-sec for no wheel coupling to approximately 377 Nm-sec. The resulting thruster control torques and momentum wheel control torque are shown in Figs. 20 and 21. Fig. 21 also includes the \hat{b}_2 momentum wheel angular rate history during the maneuver.

These results indicate that the system is well behaved in the sense that despinning and detumbling can be accomplished with relatively small control requirements, and that no violent dynamical behavior occurs even when internal control torques only are applied. Also, the use of momentum wheels to reduce thruster requirements is possible, although no evidence is presented that the wheels provide any major benefit in terms of efficient system control.

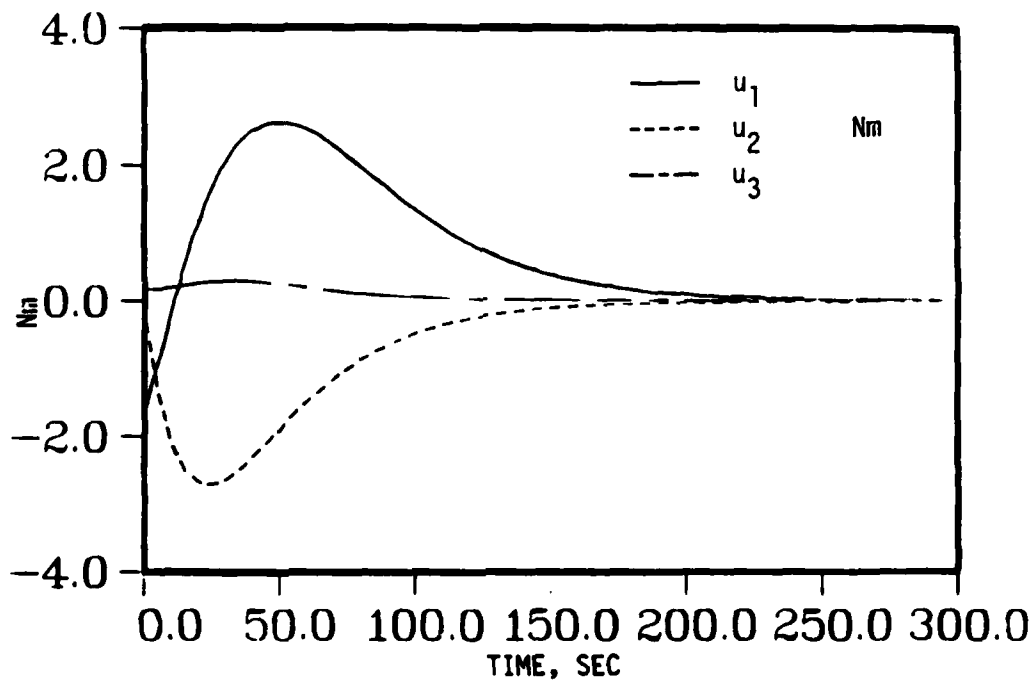


Fig. 3. OMV Thrust Torques, Momentum Wheels Uncoupled.

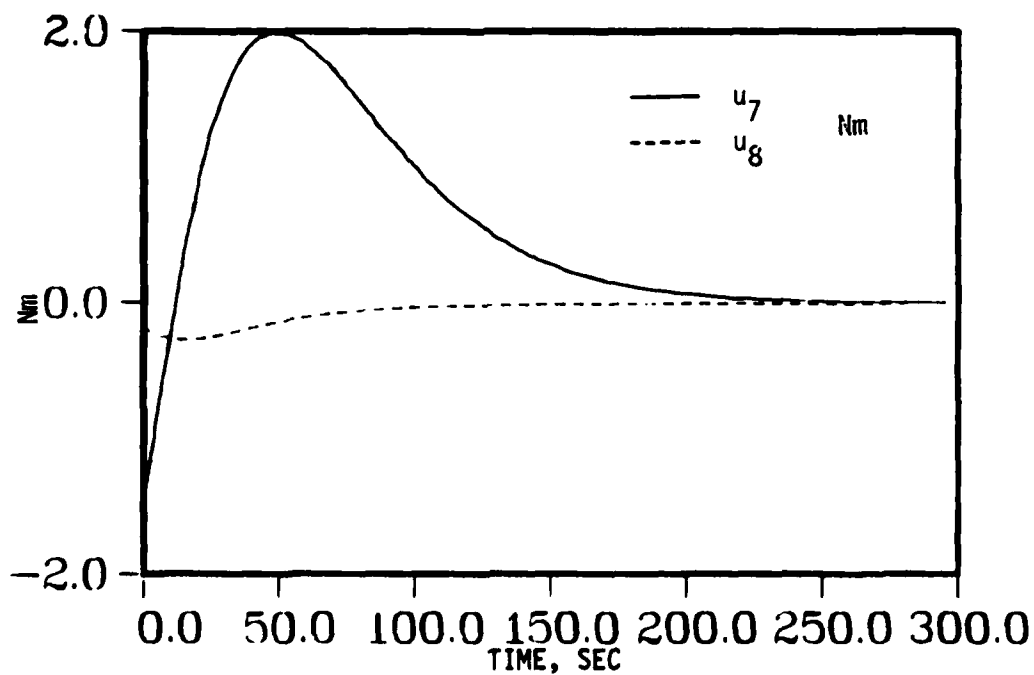


Fig. 4. Gimbal (Universal Joint) Torques, Uncoupled Momentum Wheels.

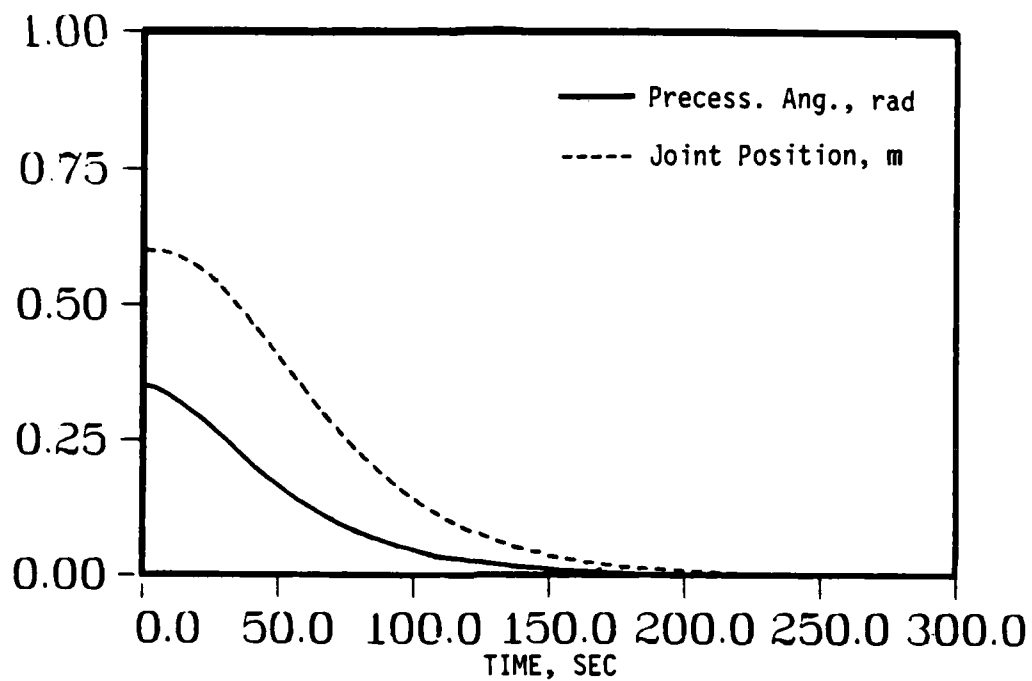


Fig. 5. Joint Position and Precession Angle Decay

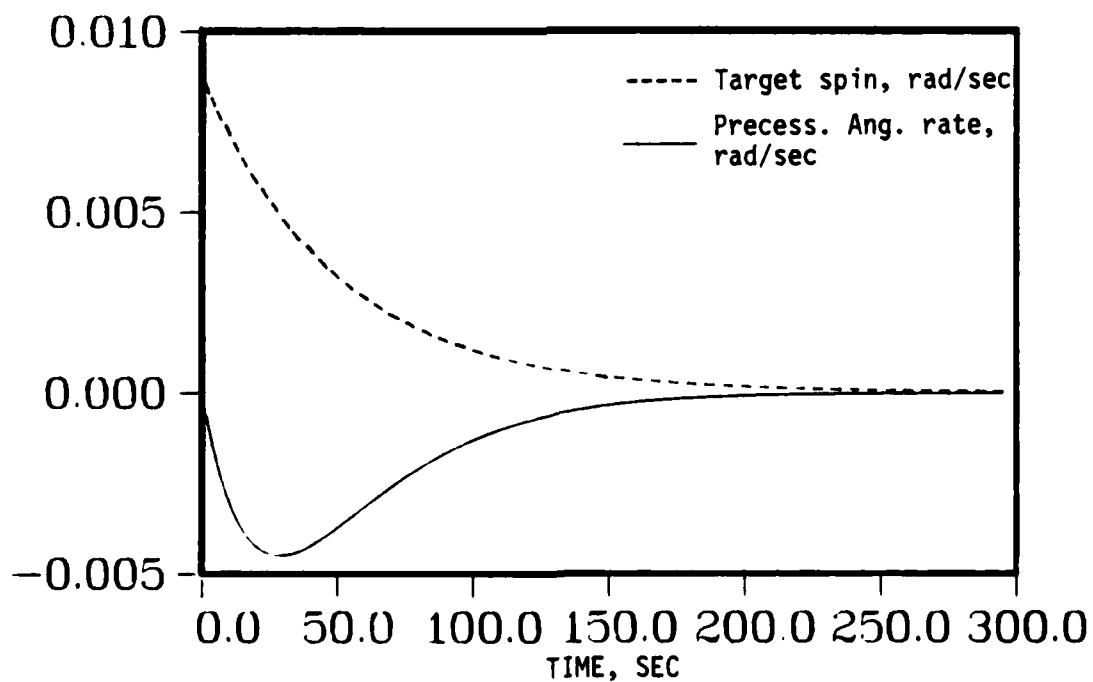


Fig. 6. Target Spin and Precession Rate Decays

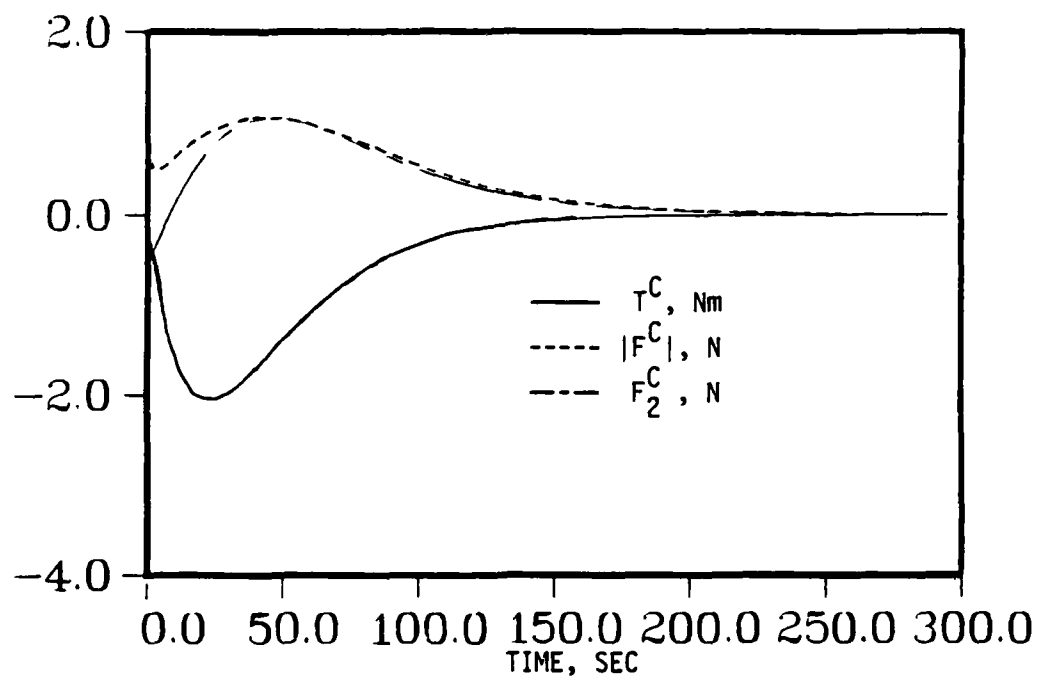


Fig. 7. Constraint Loads at Universal Joint

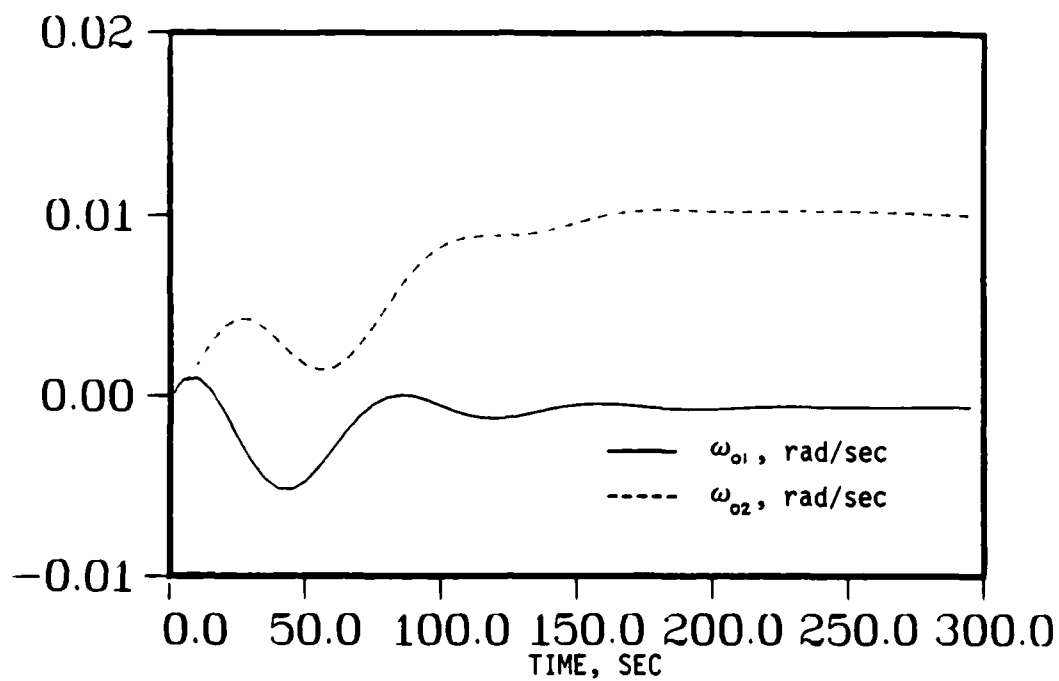


Fig. 8. Angular Velocities of OMV with u_7 and u_8 Feedback Only

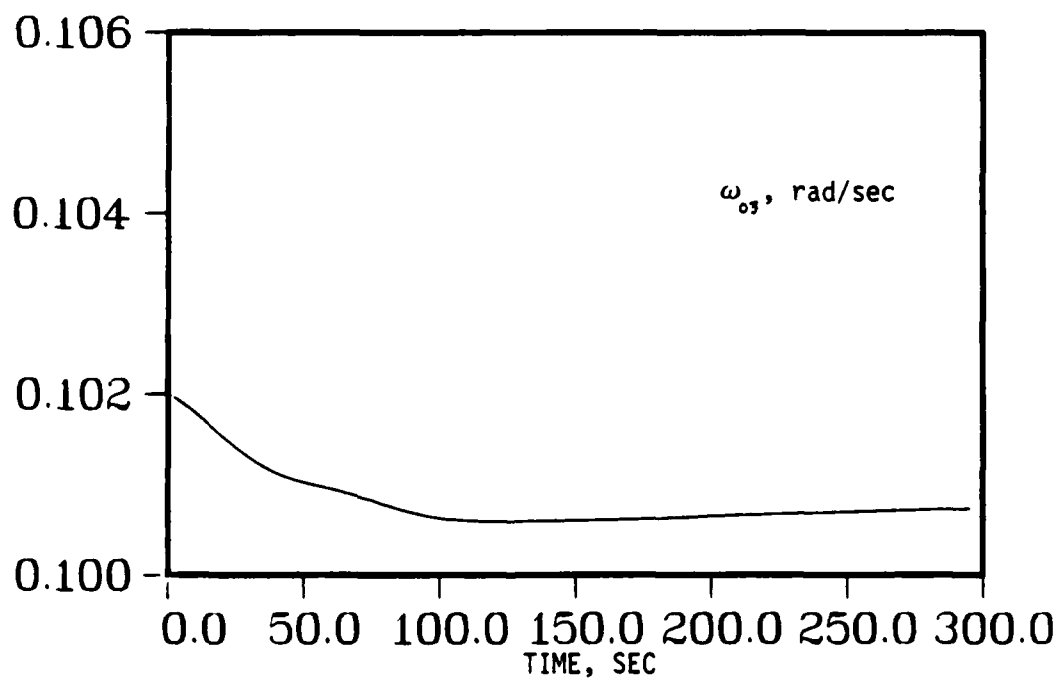


Fig. 9. Angular Velocity ω_{o3} of OMV with u_7 and u_8 Feedback Only

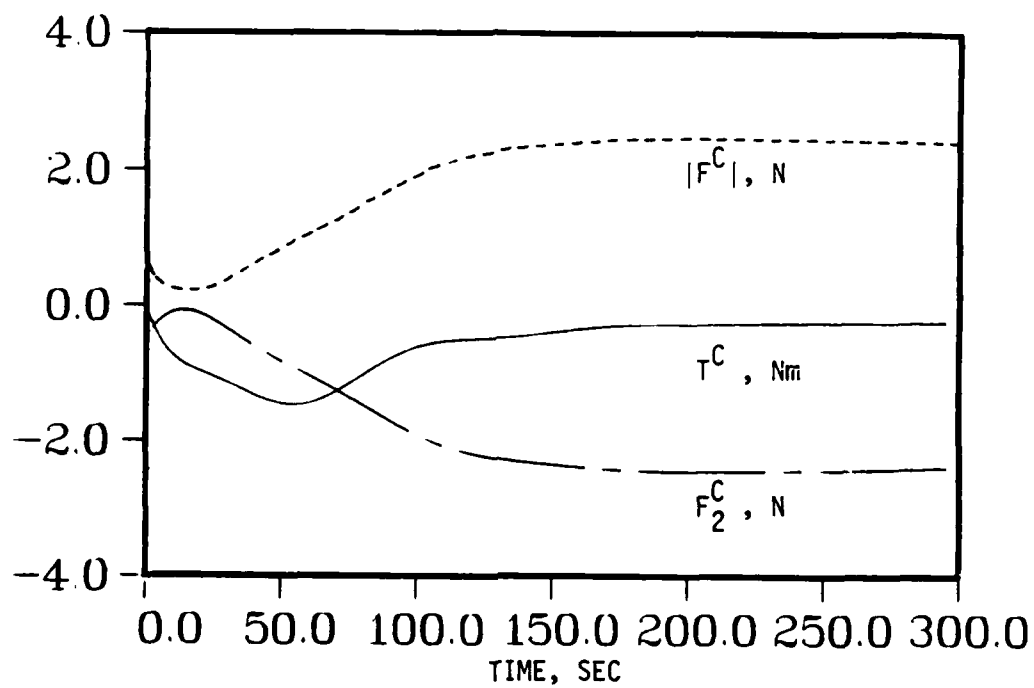


Fig. 10. Joint Constraint Loads, u_7 and u_8 Feedback Only

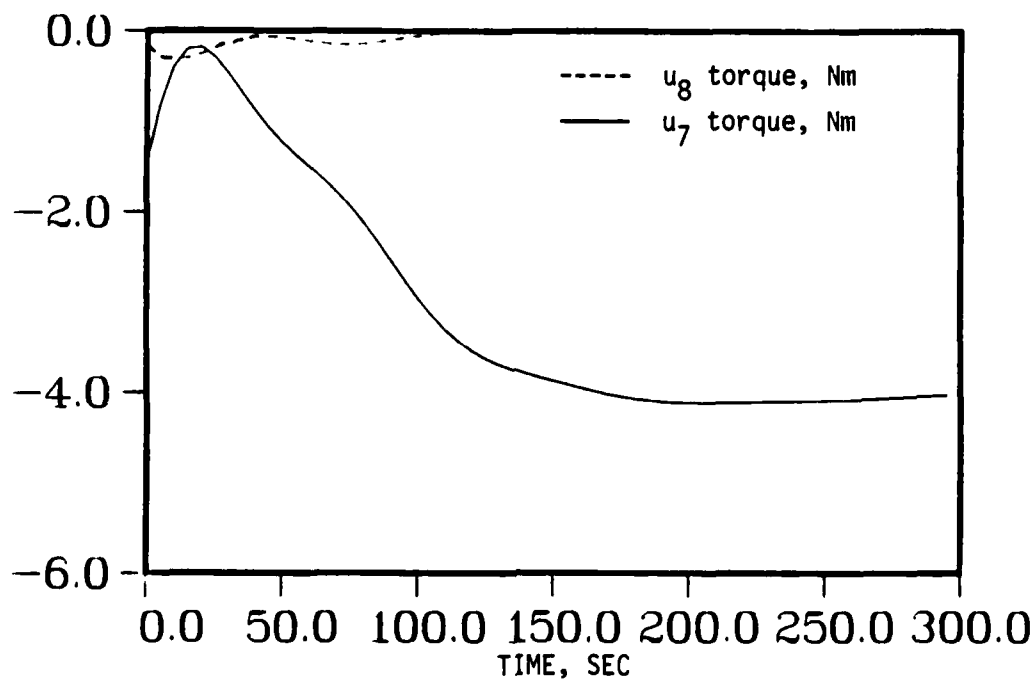


Fig. 11. Control Torque History, u_7 and u_8 Feedback Only

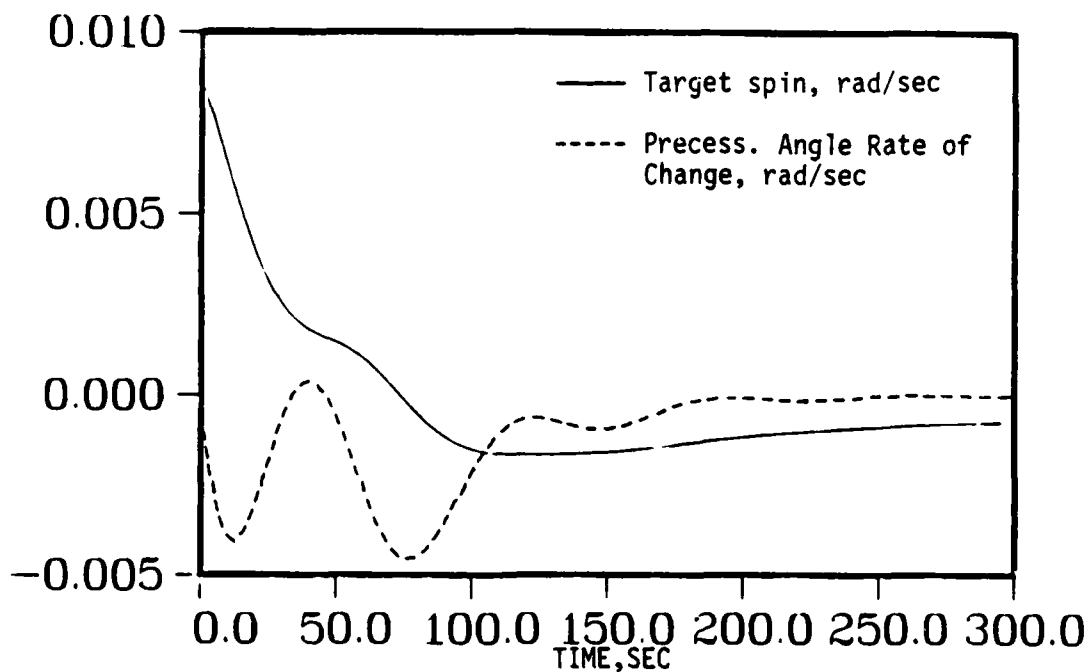


Fig. 12. Target Spin and Precession Angle Rates, u_7 and u_8 Feedback Only

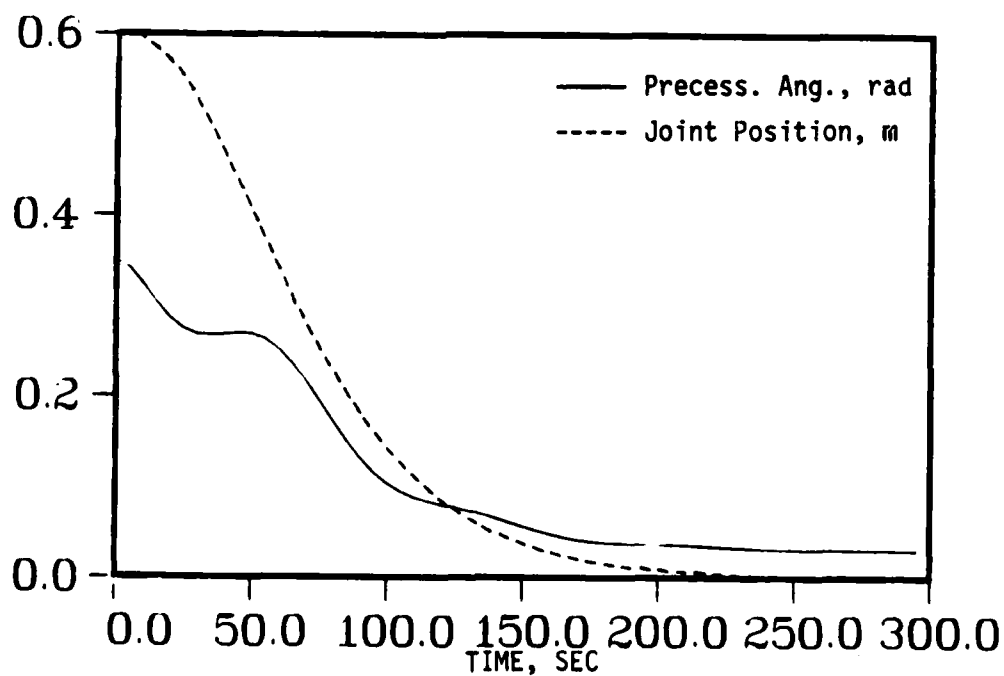


Fig. 13. Target Precession Angle and Joint Position, u_7 and u_8 Feedback Only

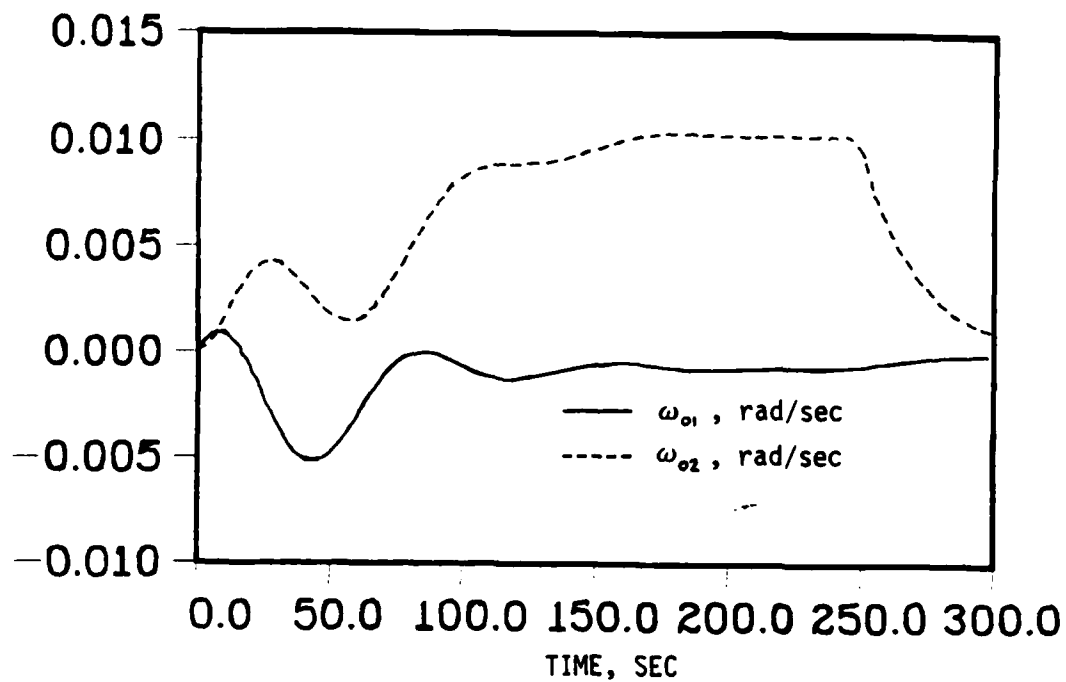


Fig. 14. OMV Angular Velocity Components; Full Feedback Added at $t = 250$ seconds

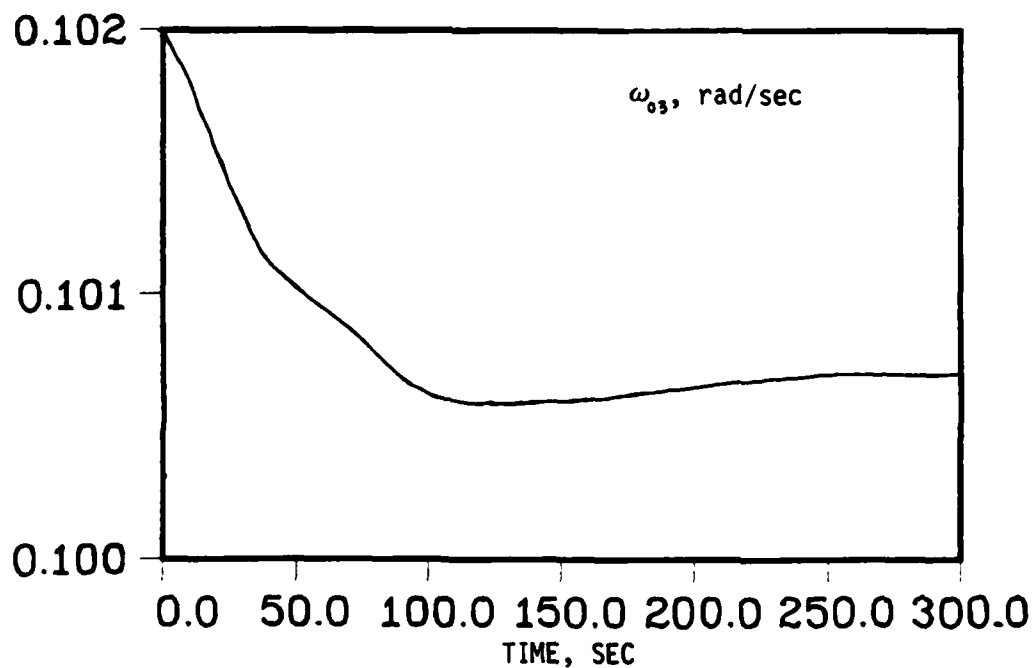


Fig. 15. OMV \hat{b}_3 Angular Velocity Component; Full Feedback Added at $t = 250$ seconds

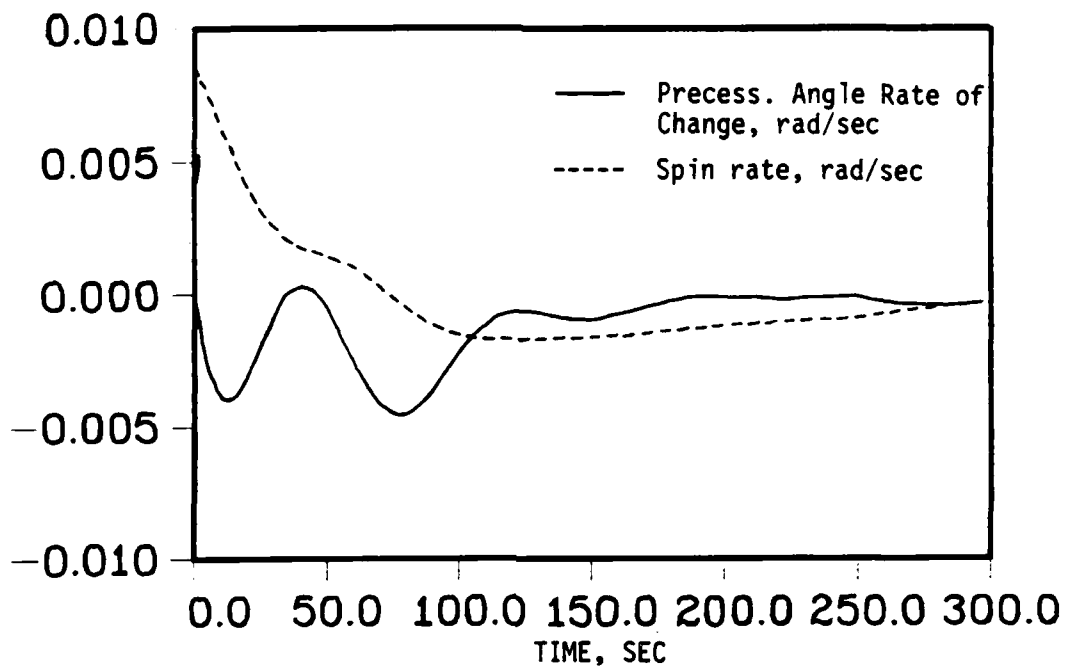


Fig. 16. Precession Angle Rate of Change and Target Spin Rate; Full Feedback Added at $t = 250$ seconds

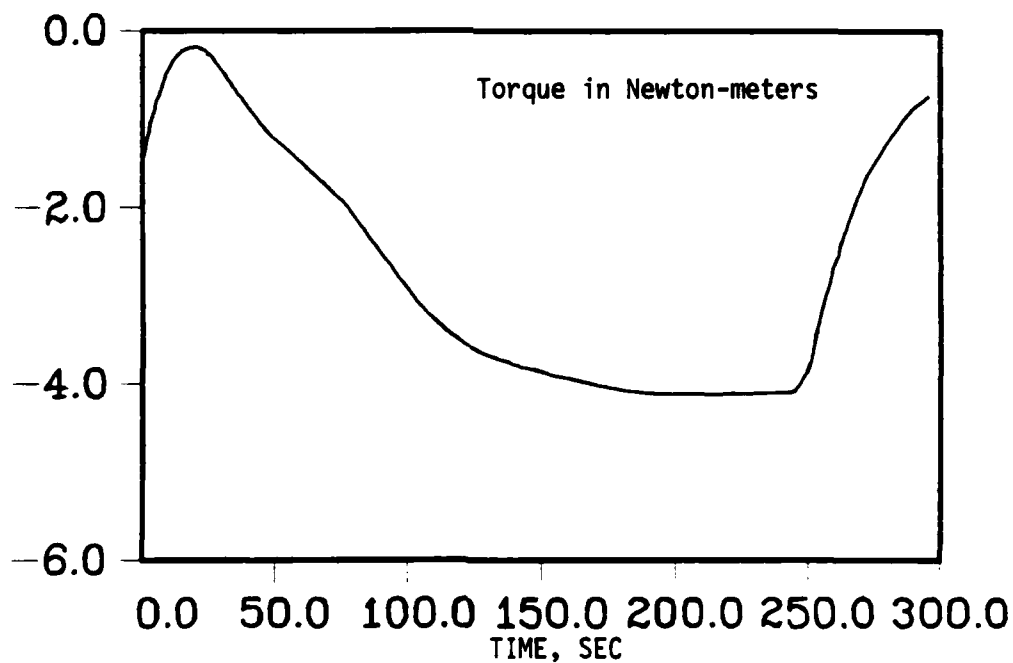


Fig. 17. Gimbal Control Torque u_7 With Full Feedback Added at $t = 250$ seconds

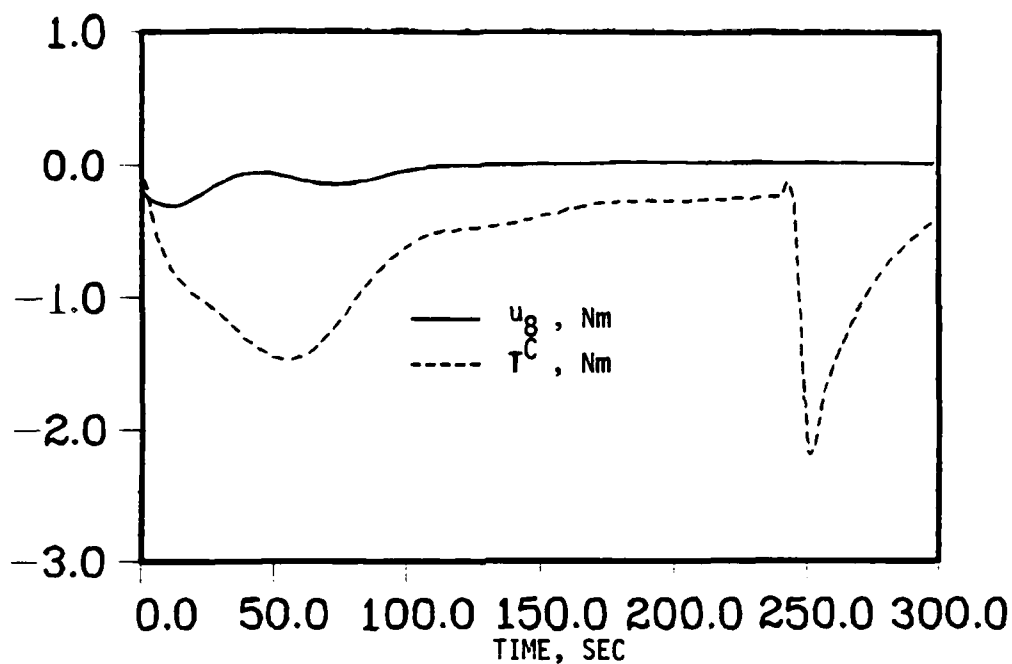


Fig. 18. Control Torque u_8 and Constraint Torque T^C ; Full Feedback at $t = 250$ seconds

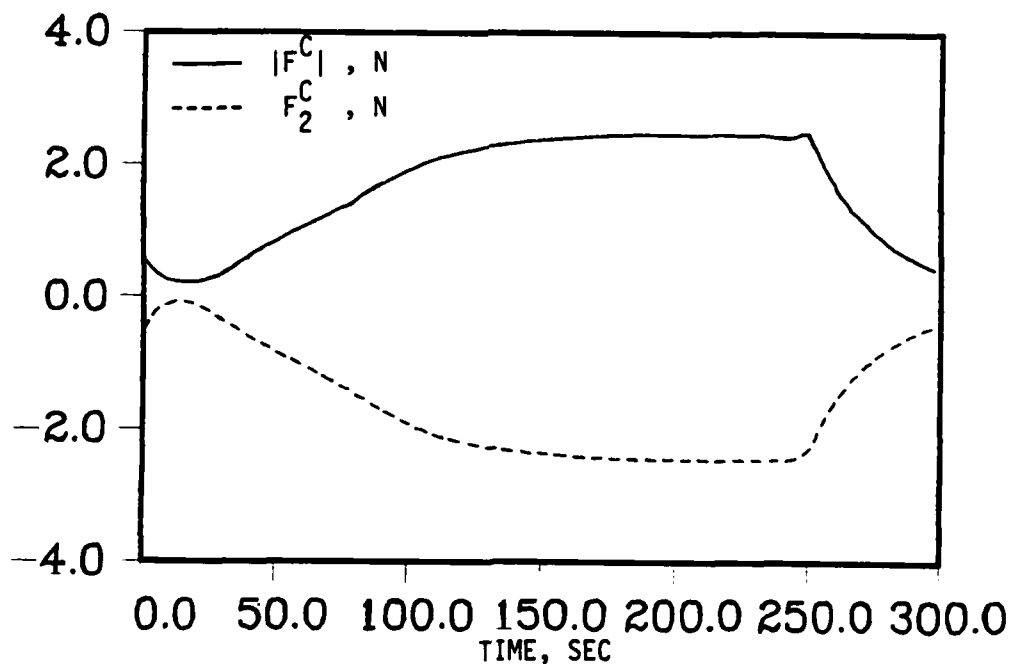


Fig. 19. Constraint Force Magnitude and b_2 Component; Full Feedback Added at $t = 250$ seconds

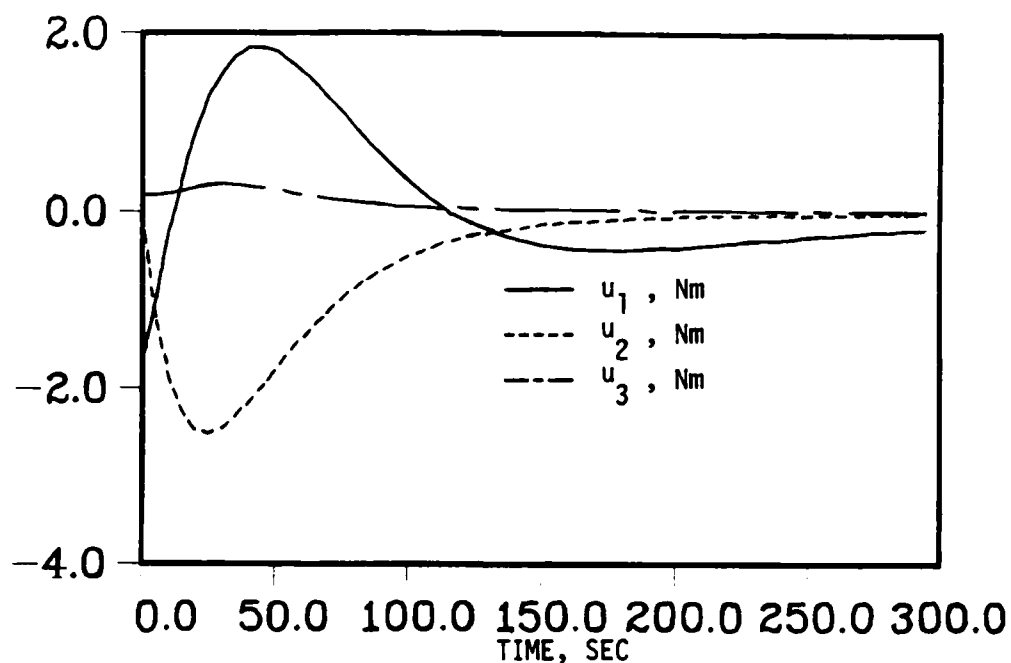


Fig. 20. OMV Thruster Torques, \hat{b}_2 Momentum Wheel Torque Coupled to Target Precession Angle

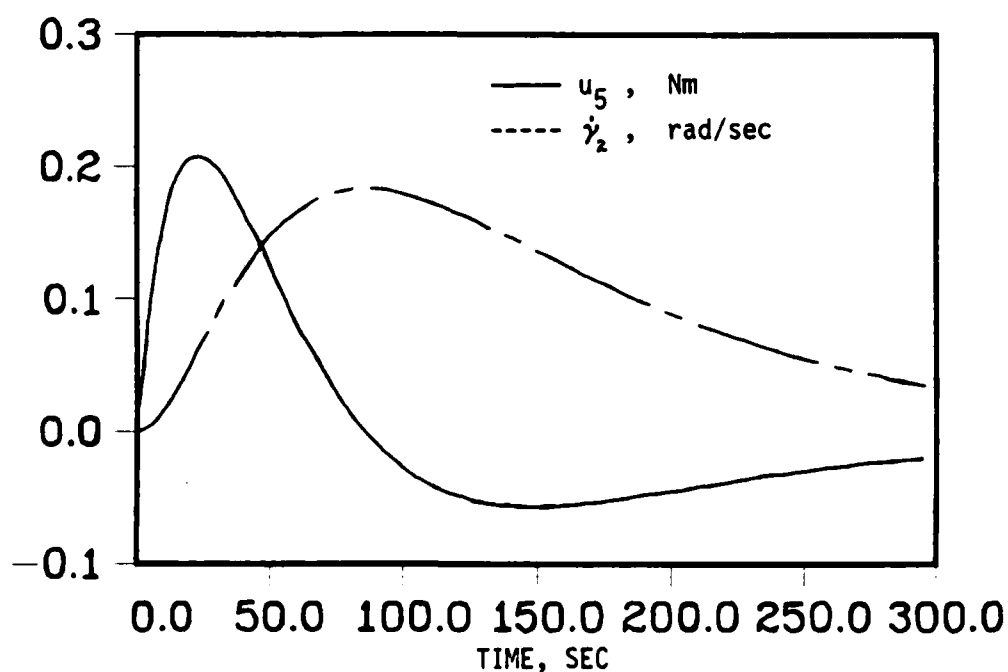


Fig. 21. \hat{b}_2 Momentum Wheel Control Torque, u_5 , and Wheel Angular Vel.; Control Torque u_5 Coupled to Precession Angle

TABLE III.

time	u_7	u_8	T^C	$ F^C $	F_2^C
0	-1.500	-.192	.000	.613	-.576
5	-.822	-.242	-.984	.503	-.225
10	-.176	-.267	-1.576	.631	.097
15	.399	-.274	-1.897	.759	.374
20	.884	-.267	-2.032	.859	.601
25	1.273	-.251	-2.043	.935	.778
30	1.568	-.230	-1.973	.993	.907
35	1.777	-.207	-1.853	1.033	.992
40	1.909	-.183	-1.705	1.056	1.041
45	1.976	-.161	-1.545	1.061	1.058
50	1.989	-.140	-1.382	1.051	1.050
55	1.959	-.121	-1.224	1.027	1.023
60	1.895	-.104	-1.076	.990	.981
65	1.808	-.090	-.939	.945	.928
70	1.703	-.077	-.815	.892	.869
75	1.588	-.067	-.704	.835	.806
80	1.468	-.058	-.606	.775	.741
85	1.346	-.050	-.520	.714	.676
90	1.226	-.043	-.445	.654	.613
95	1.109	-.038	-.380	.595	.553
100	.998	-.033	-.324	.538	.496
105	.894	-.029	-.276	.484	.443
110	.797	-.025	-.235	.434	.393
115	.708	-.022	-.200	.387	.348
120	.626	-.020	-.170	.344	.307
125	.552	-.018	-.144	.304	.270
130	.485	-.016	-.123	.268	.236
135	.425	-.014	-.104	.236	.207
140	.371	-.012	-.089	.207	.180
145	.323	-.011	-.076	.181	.156
150	.281	-.010	-.064	.157	.136
155	.244	-.009	-.055	.137	.117
160	.211	-.008	-.047	.119	.101
165	.182	-.007	-.040	.103	.087
170	.157	-.007	-.034	.089	.075
175	.135	-.006	-.029	.077	.064
180	.116	-.005	-.025	.066	.055
185	.100	-.005	-.022	.057	.047
190	.085	-.004	-.019	.049	.040
195	.073	-.004	-.016	.042	.034
200	.062	-.004	-.014	.035	.029
205	.053	-.003	-.012	.030	.025
210	.045	-.003	-.010	.026	.021
215	.038	-.003	-.009	.022	.018
220	.033	-.002	-.008	.019	.015
225	.028	-.002	-.007	.016	.013
230	.023	-.002	-.006	.013	.011

TABLE III., cont'd

time	u_7	u_8	T^C	$ F^C $	F_2^C
235	.020	-.002	-.005	.011	.009
240	.017	-.002	-.004	.010	.008
245	.014	-.001	-.004	.008	.006
250	.012	-.001	-.003	.007	.005
255	.010	-.001	-.003	.006	.005
260	.008	-.001	-.002	.005	.004
265	.007	-.001	-.002	.004	.003
270	.006	-.001	-.002	.003	.003
275	.005	-.001	-.002	.003	.002
280	.004	-.001	-.001	.002	.002
285	.004	-.001	-.001	.002	.002
290	.003	-.001	-.001	.002	.001
295	.002	-.001	-.001	.001	.001
??					

Note: This table of universal joint control torques and constraint loads applies to the case of feedback control with uncoupled momentum wheels.

TABLE IV.

time	u_7	u_8	T^C	$ F^C $	F_2^C
0	-1.500	-.192	.000	.613	-.576
5	-.822	-.242	-.984	.503	-.225
10	-.176	-.267	-1.576	.631	.097
15	.399	-.274	-1.897	.759	.374
20	.884	-.267	-2.032	.859	.601
25	1.273	-.251	-2.043	.935	.778
30	1.568	-.230	-1.973	.993	.907
35	1.777	-.207	-1.853	1.033	.992
40	1.909	-.183	-1.705	1.056	1.041
45	1.976	-.161	-1.545	1.061	1.058
50	1.989	-.140	-1.382	1.051	1.050
55	1.959	-.121	-1.224	1.027	1.023
60	1.895	-.104	-1.076	.990	.981
65	1.808	-.090	-.939	.945	.928
70	1.703	-.077	-.815	.892	.869
75	1.588	-.067	-.704	.835	.806
80	1.468	-.058	-.606	.775	.741
85	1.346	-.050	-.520	.714	.676
90	1.226	-.043	-.445	.654	.613
95	1.109	-.038	-.380	.595	.553
100	.998	-.033	-.324	.538	.496
105	.894	-.029	-.276	.484	.443
110	.797	-.025	-.235	.434	.393
115	.708	-.022	-.200	.387	.348
120	.626	-.020	-.170	.344	.307
125	.552	-.018	-.144	.304	.270
130	.485	-.016	-.123	.268	.236
135	.425	-.014	-.104	.236	.207
140	.371	-.012	-.089	.207	.180
145	.323	-.011	-.076	.181	.156
150	.281	-.010	-.064	.157	.136
155	.244	-.009	-.055	.137	.117
160	.211	-.008	-.047	.119	.101
165	.182	-.007	-.040	.103	.087
170	.157	-.007	-.034	.089	.075
175	.135	-.006	-.029	.077	.064
180	.116	-.005	-.025	.066	.055
185	.100	-.005	-.022	.057	.047
190	.085	-.004	-.019	.049	.040
195	.073	-.004	-.016	.042	.034
200	.062	-.004	-.014	.035	.029
205	.053	-.003	-.012	.030	.025
210	.045	-.003	-.010	.026	.021
215	.038	-.003	-.009	.022	.018
220	.033	-.002	-.008	.019	.015
225	.028	-.002	-.007	.016	.013
230	.023	-.002	-.006	.013	.011

TABLE IV. cont'd

time	u_7	u_8	T^C	$ F^C $	F_2^C
235	.020	-.002	-.005	.011	.009
240	.017	-.002	-.004	.010	.008
245	.014	-.001	-.004	.008	.006
250	.012	-.001	-.003	.007	.005
255	.010	-.001	-.003	.006	.005
260	.008	-.001	-.002	.005	.004
265	.007	-.001	-.002	.004	.003
270	.006	-.001	-.002	.003	.003
275	.005	-.001	-.002	.003	.002
280	.004	-.001	-.001	.002	.002
285	.004	-.001	-.001	.002	.002
290	.003	-.001	-.001	.002	.001
295	.002	-.001	-.001	.001	.001
??					

Note: This table of universal joint control torques and constraint loads applies to the case of feedback control with the b_2 momentum wheel coupled.

TABLE V.

time	u_1	u_2	u_3	u_5	2
0	-1.732	-.066	.180	.000	.000
5	-.960	-1.209	.182	.096	.005
10	-.242	-1.906	.205	.157	.016
15	.382	-2.296	.238	.191	.032
20	.893	-2.473	.269	.206	.051
25	1.286	-2.504	.291	.207	.069
30	1.566	-2.438	.301	.199	.088
35	1.744	-2.311	.299	.184	.105
40	1.832	-2.147	.287	.165	.121
45	1.845	-1.964	.268	.145	.135
50	1.799	-1.777	.244	.123	.148
55	1.706	-1.593	.218	.102	.158
60	1.579	-1.418	.192	.082	.166
65	1.430	-1.256	.167	.062	.173
70	1.267	-1.108	.144	.045	.178
75	1.098	-.974	.122	.028	.181
80	.929	-.855	.104	.014	.183
85	.764	-.750	.088	.001	.183
90	.607	-.657	.074	-.010	.183
95	.461	-.576	.062	-.019	.182
100	.325	-.506	.052	-.028	.180
105	.203	-.445	.044	-.035	.177
110	.093	-.392	.037	-.040	.173
115	-.005	-.346	.032	-.045	.169
120	-.090	-.306	.027	-.048	.165
125	-.163	-.271	.023	-.051	.161
130	-.226	-.242	.020	-.053	.156
135	-.278	-.216	.017	-.055	.151
140	-.322	-.194	.015	-.056	.146
145	-.357	-.174	.013	-.056	.141
150	-.385	-.157	.011	-.056	.136
155	-.406	-.142	.010	-.056	.131
160	-.422	-.129	.009	-.055	.126
165	-.433	-.118	.008	-.054	.121
170	-.439	-.108	.007	-.053	.116
175	-.441	-.099	.006	-.052	.111
180	-.441	-.091	.006	-.051	.106
185	-.437	-.084	.005	-.049	.102
190	-.432	-.077	.004	-.048	.097
195	-.424	-.072	.004	-.046	.093
200	-.416	-.067	.004	-.045	.089
205	-.405	-.062	.003	-.043	.085
210	-.394	-.058	.003	-.041	.081
215	-.383	-.054	.003	-.040	.077
220	-.371	-.050	.002	-.038	.074
225	-.358	-.047	.002	-.037	.070
230	-.345	-.044	.002	-.035	.067

TABLE V. cont'd

time	u_1	u_2	u_3	u_5	2
235	-.333	-.041	.002	-.034	.064
240	-.320	-.039	.002	-.032	.061
245	-.307	-.037	.001	-.031	.058
250	-.295	-.035	.001	-.030	.055
255	-.283	-.033	.001	-.028	.053
260	-.271	-.031	.001	-.027	.050
265	-.259	-.029	.001	-.026	.048
270	-.248	-.027	.001	-.025	.046
275	-.237	-.026	.001	-.023	.043
280	-.226	-.024	.001	-.022	.041
285	-.216	-.023	.001	-.021	.039
290	-.206	-.022	.001	-.020	.037
295	-.197	-.021	.001	-.019	.036
??					

Note: This table of thruster torques u_1 , u_2 , and u_3 and wheel torque u_5 applies to the case of feedback control with the b_2 momentum wheel coupled.

TABLE VI.

time	u_7	u_8	T^C	$ F^C $	F_2^C
0	-1.500	-.192	.021	.612	-.500
5	-.830	-.281	-.471	.340	-.225
10	-.403	-.314	-.738	.242	-.094
15	-.201	-.298	-.882	.223	-.071
20	-.180	-.251	-.974	.237	-.124
25	-.285	-.192	-1.054	.288	-.223
30	-.463	-.136	-1.139	.379	-.346
35	-.671	-.093	-1.231	.495	-.476
40	-.878	-.068	-1.323	.619	-.602
45	-1.067	-.063	-1.402	.740	-.721
50	-1.230	-.074	-1.454	.851	-.831
55	-1.371	-.095	-1.470	.953	-.936
60	-1.499	-.119	-1.444	1.051	-1.038
65	-1.629	-.139	-1.379	1.150	-1.141
70	-1.771	-.151	-1.280	1.253	-1.248
75	-1.933	-.151	-1.159	1.363	-1.359
80	-2.119	-.141	-1.029	1.478	-1.473
85	-2.322	-.122	-.900	1.596	-1.589
90	-2.537	-.099	-.784	1.712	-1.704
95	-2.751	-.075	-.687	1.822	-1.813
100	-2.954	-.054	-.612	1.922	-1.914
105	-3.139	-.036	-.559	2.012	-2.003
110	-3.300	-.024	-.524	2.088	-2.080
115	-3.433	-.016	-.504	2.152	-2.143
120	-3.541	-.011	-.492	2.204	-2.194
125	-3.626	-.010	-.483	2.245	-2.235
130	-3.693	-.010	-.473	2.279	-2.268
135	-3.746	-.010	-.458	2.306	-2.295
140	-3.792	-.010	-.440	2.330	-2.318
145	-3.834	-.009	-.416	2.351	-2.338
150	-3.873	-.008	-.391	2.371	-2.357
155	-3.912	-.005	-.364	2.389	-2.375
160	-3.950	-.003	-.340	2.407	-2.392
165	-3.986	.000	-.318	2.423	-2.408
170	-4.020	.003	-.301	2.437	-2.422
175	-4.049	.005	-.288	2.449	-2.434
180	-4.072	.006	-.280	2.458	-2.443
185	-4.090	.007	-.276	2.465	-2.449
190	-4.103	.007	-.274	2.469	-2.453
195	-4.110	.006	-.273	2.471	-2.455
200	-4.113	.006	-.272	2.471	-2.455
205	-4.114	.005	-.271	2.470	-2.454
210	-4.112	.004	-.269	2.469	-2.452
215	-4.110	.003	-.266	2.466	-2.450
220	-4.107	.003	-.262	2.464	-2.447
225	-4.104	.003	-.258	2.461	-2.445
230	-4.101	.003	-.253	2.459	-2.442

TABLE VI. cont'd

time	u_7	u_8	T^C	$ F^C $	F_2^C
235	-4.099	.003	-.249	2.456	-2.440
240	-4.096	.003	-.246	2.453	-2.437
245	-4.093	.003	-.243	2.450	-2.434
250	-3.847	.003	-2.162	2.495	-2.284
255	-3.192	.003	-1.813	2.072	-1.896
260	-2.643	.004	-1.519	1.720	-1.572
265	-2.194	.005	-1.276	1.432	-1.306
270	-1.824	.005	-1.075	1.194	-1.087
275	-1.519	.006	-.907	.998	-.906
280	-1.267	.006	-.768	.836	-.757
285	-1.059	.006	-.651	.702	-.634
290	-.887	.006	-.553	.590	-.532
295	-.743	.006	-.471	.497	-.446
??					

Note: This table of universal joint control torques and constraint loads applies to the case of feedback with control torques u_7 and u_8 only until $t = 250$ seconds, at which time the complete control vector u is fed back.

TABLE VII.

time	ω_{01}	ω_{02}	ω_{03}	\dot{y}_4	\dot{y}_5
0	.000	.000	.102	.000	.009
5	.001	.001	.102	-.003	.008
10	.001	.002	.102	-.004	.006
15	.000	.003	.102	-.004	.005
20	-.001	.004	.102	-.003	.004
25	-.002	.004	.101	-.002	.003
30	-.004	.004	.101	-.001	.003
35	-.005	.004	.101	.000	.002
40	-.005	.003	.101	.000	.002
45	-.005	.002	.101	.000	.002
50	-.005	.002	.101	-.001	.001
55	-.004	.001	.101	-.002	.001
60	-.003	.002	.101	-.003	.001
65	-.002	.002	.101	-.004	.001
70	-.001	.003	.101	-.004	.000
75	.000	.004	.101	-.005	.000
80	.000	.005	.101	-.004	-.001
85	.000	.006	.101	-.004	-.001
90	.000	.007	.101	-.004	-.001
95	.000	.008	.101	-.003	-.001
100	-.001	.008	.101	-.002	-.002
105	-.001	.009	.101	-.002	-.002
110	-.001	.009	.101	-.001	-.002
115	-.001	.009	.101	-.001	-.002
120	-.001	.009	.101	-.001	-.002
125	-.001	.009	.101	-.001	-.002
130	-.001	.009	.101	-.001	-.002
135	-.001	.009	.101	-.001	-.002
140	-.001	.009	.101	-.001	-.002
145	-.001	.009	.101	-.001	-.002
150	-.001	.010	.101	-.001	-.002
155	.000	.010	.101	-.001	-.002
160	.000	.010	.101	-.001	-.002
165	-.001	.010	.101	-.001	-.001
170	-.001	.010	.101	.000	-.001
175	-.001	.010	.101	.000	-.001
180	-.001	.010	.101	.000	-.001
185	-.001	.010	.101	.000	-.001
190	-.001	.010	.101	.000	-.001
195	-.001	.010	.101	.000	-.001
200	-.001	.010	.101	.000	-.001
205	-.001	.010	.101	.000	-.001
210	-.001	.010	.101	.000	-.001
215	-.001	.010	.101	.000	-.001
220	-.001	.010	.101	.000	-.001
225	-.001	.010	.101	.000	-.001
230	-.001	.010	.101	.000	-.001

TABLE VII. cont'd

time	ω_{01}	ω_{02}	ω_{03}	γ_4	γ_5
235	-.001	.010	.101	.000	-.001
240	-.001	.010	.101	.000	-.001
245	-.001	.010	.101	.000	-.001
250	-.001	.009	.101	.000	-.001
255	.000	.008	.101	.000	-.001
260	.000	.006	.101	.000	-.001
265	.000	.005	.101	.000	-.001
270	.000	.004	.101	.000	-.001
275	.000	.003	.101	.000	-.001
280	.000	.002	.101	.000	.000
285	.000	.002	.101	.000	.000
290	.000	.002	.101	.000	.000
295	.000	.001	.101	.000	.000
??					

NOTE: This table of OMV angular velocity components, target spin rate and precession angle rate of change is for the case of feedback with u_7 and u_8 control vector components only, until $t = 250$ seconds when control is with the complete u vector.

V. Conclusion

A nonlinear feedback control law was developed and used to despin and detumble an axially symmetric target satellite originally in steady spin and precession. The control law derivation is based upon Liapunov stability theory, and ensures the global asymptotic stability of the final spin-stabilized equilibrium state. The results indicate that the system is well behaved, in the sense that changes in both the system state and in the control torques are smooth throughout the maneuver. The control torque magnitudes are relatively small, and no extreme loading of the connecting joint between OMV and target satellites occurred. The system could be driven very close to the spin-stabilized state using the joint control torques alone. However, a residual target precession angle remained at the end of the 300 second maneuver, as did non-zero b_1 and b_2 OMV velocity components. This is due to the fact that after approximately 200 seconds of feedback control, the matrix, A , of Eq (26) is nearly diagonal, and as a result the control torques u_7 and u_8 are coupled strongly only to the target precession angle rate and spin rate, and the precession angle (states x_7 , x_8 , and x_9), all of which have very small values. The available control torques at the universal joint are thus insufficient for the reduction of target precession angle at any appreciable rate. Implementation of full vector control (using all eight control torques) at $t = 250$ seconds successfully drove the system to the spin-stabilized equilibrium.

Although the OMV thrust torque magnitude could be reduced by coupling a momentum wheel torque to the target precession angle, no attempt was made to accomplish detumbling with momentum wheel and joint

torques alone. Any attempt made to couple the b_3 momentum wheel with system states x_7 or x_8 resulted in an increase in at least one thrust torque profile, with no obvious positive influence on system behavior.

A follow on effort might concentrate on the development of a reliable technique for determining the values of the off-diagonal gain matrix terms, based on desired system response. Then an attempt could be made to perform the bulk of the maneuver using only internal torques.

References

1. Conway, B.A., and Widhalm, J.W., "Optimal Continuous Control for Remote Orbital Capture," AIAA J. of Guidance, Control, and Dynamics, to appear.
2. Fletcher, H.J., Rongved, L., and Yu, E.Y., "Dynamics Analysis of a Two-Body Gravitationally Oriented Satellite," Bell System Tech. J., Vol. 42, No. 5 (1963) 2239-2266.
3. Hooker, W.W., and Margulies, G., "The Dynamical Attitude Equations for an n-Body Satellite," J. of the Astronautical Sciences, Vol. 12, No. 4 (Winter, 1965) 123-128.
4. Hooker, W.W., "A Set of r Dynamical Attitude Equations for an Arbitrary n-Body Satellite Having r Rotational Degrees of Freedom," AIAA J., Vol. 8, No. 7 (1970) 1205-1207.
5. Conway, B.A., and Widhalm, J.W., "Equations of Attitude Motion for an n-Body Satellite With Moving Joints," AIAA J. of Guidance, Control, and Dynamics, Vol. 8, No.4 (1985) 537-539.
6. Greenwood, D.T., Principles of Dynamics. Prentice-Hall, Inc., Englewood Cliffs, NJ, 1965.
7. Widhalm, J.W., and Conway, B.A., "Nonlinear Feedback Control for Remote Orbital Capture," paper No. AAS85-368 presented at AAS/AIAA Astrodynamics Specialist Conference. AAS Publications Office, PO Box 28130, San Diego, CA (August 1985).
8. Vidyasagar, M., Nonlinear Systems Analysis. Prentice-Hall, Inc., Englewood Cliffs, NJ, 1978.
9. Widhalm, J.W., "Optimal Open Loop and Nonlinear Feedback Control for Remote Orbital Capture," Ph.D. Thesis, University of Illinois at Urbana-Champaign, 1985.

VITA

Lieutenant Kirk R. Fleming was born on 13 October 1954 in Port Huron, Michigan. He graduated from Port Huron Northern High School in January 1972, and attended the University of Texas at Austin from August 1979 to December 1981, when he received the degree of Bachelor of Science in Aerospace Engineering. He received a commission in the USAF through the Air Force Officer Training School in April 1982. He then served as a research and development project engineer in the Air Force Flight Dynamics Laboratory, Vehicle Equipment Division, Wright-Patterson AFB, Ohio until entering the School of Engineering, Air Force Institute of Technology, in May 1984.

Permanent address : 1954 Burns Road

Smith's Creek, MI 48074

UNCLASSIFIED

SECURITY CLASSIFICATION OF THIS PAGE

REPORT DOCUMENTATION PAGE

1a. REPORT SECURITY CLASSIFICATION UNCLASSIFIED			1b. RESTRICTIVE MARKINGS		
2a. SECURITY CLASSIFICATION AUTHORITY			3. DISTRIBUTION/AVAILABILITY OF REPORT Approved for public release; Distribution unlimited		
2b. DECLASSIFICATION/DOWNGRADING SCHEDULE					
4. PERFORMING ORGANIZATION REPORT NUMBER(S) AFIT/GA/AA/85D-5			5. MONITORING ORGANIZATION REPORT NUMBER(S)		
6a. NAME OF PERFORMING ORGANIZATION School of Engineering AFIT		6b. OFFICE SYMBOL (If applicable)		7a. NAME OF MONITORING ORGANIZATION	
6c. ADDRESS (City, State and ZIP Code) Air Force Institute of Technology Wright-Patterson AFB, OH 45433			7b. ADDRESS (City, State and ZIP Code)		
8a. NAME OF FUNDING/SPONSORING ORGANIZATION		8b. OFFICE SYMBOL (If applicable)		9. PROCUREMENT INSTRUMENT IDENTIFICATION NUMBER	
8c. ADDRESS (City, State and ZIP Code)			10. SOURCE OF FUNDING NOS.		
			PROGRAM ELEMENT NO.		PROJECT NO.
			TASK NO.		WORK UNIT NO.
11. TITLE (Include Security Classification) See block 19					
12. PERSONAL AUTHOR(S) Fleming, Kirk R., 1Lt, USAF					
13a. TYPE OF REPORT MS Thesis		13b. TIME COVERED FROM _____ TO _____		14. DATE OF REPORT (Yr., Mo., Day) 13 Dec 85	
15. PAGE COUNT 59					
16. SUPPLEMENTARY NOTATION					
17. COSATI CODES			18. SUBJECT TERMS (Continue on reverse if necessary and identify by block number)		
FIELD	GROUP	SUB. GR.			
22	02		satellite, dynamics, teleoperator, orbital capture		
			docking, detumbling, despinning, feedback control		
19. ABSTRACT (Continue on reverse if necessary and identify by block number)					
<p>Title: THE DETUMBLING OF AN AXIALLY SYMMETRIC SATELLITE WITH AN ORBITAL MANEUVERING VEHICLE BY NONLINEAR FEEDBACK CONTROL</p> <p>Thesis Advisor: Lt. Col. Joseph W. Widhalm</p> <p style="text-align: right;"> <i>Approved for public release</i> LAW AFR 128-17 Lynn E. Wolaver 16 JAN 86 Dean for Research and Professional Development Air Force Institute of Technology (AFIT) Wright-Patterson AFB OH 45433 </p>					
20. DISTRIBUTION/AVAILABILITY OF ABSTRACT UNCLASSIFIED/UNLIMITED <input checked="" type="checkbox"/> SAME AS RPT. <input type="checkbox"/> DTIC USERS <input type="checkbox"/>			21. ABSTRACT SECURITY CLASSIFICATION UNCLASSIFIED		
22a. NAME OF RESPONSIBLE INDIVIDUAL Lt. Col. Joseph W. Widhalm			22b. TELEPHONE NUMBER (Include Area Code) (513) 255-5533		22c. OFFICE SYMBOL AFIT/ENY

DD FORM 1473, 83 APR

EDITION OF 1 JAN 73 IS OBSOLETE.

UNCLASSIFIED
SECURITY CLASSIFICATION OF THIS PAGE

From Block 19:

The problem of detumbling a freely spinning and precessing axially symmetric satellite is considered. Detumbling is achieved with another axisymmetric orbital maneuvering vehicle (OMV) joined to the target satellite with a universal joint. The joint provides two rotational degrees of freedom and is translated across the surface of the OMV during the detumbling process. The target satellite and the OMV with its three momentum wheels are modelled as a five body system using Eulerian-based equations of motion developed by Hooker and Margulies. A Liapunov technique is applied to derive a nonlinear feedback control law which drives the system asymptotically to a final spin-stabilized state. State and control histories are presented and indicate that the detumbling process is benign. Constraint force and moment loads at the connection between the OMV and target satellites are also presented, and indicate that no extreme loads are encountered during the despinning and detumbling process.

END

FILMED

3 - 86

DTIC